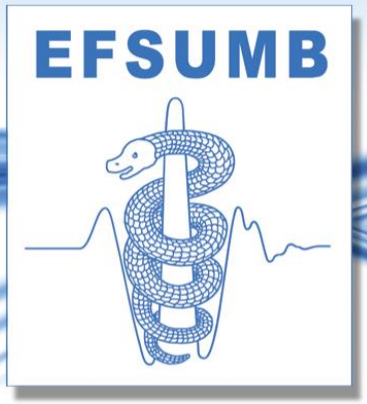

EFSUMB Course Book, 2nd Edition

Editor: Christoph F. Dietrich

Ultrasound evaluation of cerebrovascular steno-occlusive disease

Sergio Castellani[1], Boris Brkljačić[2], Laurence Needleman[3], Colin Deane[4], Fabrizio D'Abate[5], Eleonora A.M.Lucente[1] Christoph F. Dietrich[6]

[1]Department of Medical and Surgical Critical Care A.O.-U. Careggi, University of Florence, Florence, Italy. [2]Department of Diagnostic and Interventional Radiology, University Hospital "Dubrava", Medical School, University of Zagreb, Zagreb, Croatia. [3]Department of Radiology, Sidney Kimmel Medical College, Thomas Jefferson University, Philadelphia, Pennsylvania, USA. [4]Department of Vascular Surgery-Vascular Institute, St George's University Hospital, London, UK. [5]Department of Medical Engineering and Physics, King's College, London, UK. [6]Caritas-Krankenhaus Bad Mergentheim, Bad Mergentheim, Germany.

Corresponding Author:

Prof. Dr. Christoph F. Dietrich, MBA

Medizinische Klinik 2, Caritas-Krankenhaus, Uhlandstr. 7, 97980 Bad Mergentheim

Tel.: (+) 49 - 7931 – 58 – 2201. Fax: (+) 49 - 7931 – 58 – 2290

Email: christoph.dietrich@ckbm.de

Carotid arteries

Introduction

The publication of the results of the European Carotid Surgery Trial (ECST) [(1)] and the North American Symptomatic Carotid Endarterectomy Trial (NASCET) [(2)] have highlighted the existence of a close link between the degree of carotid stenosis and the risk of stroke and the importance of accurate assessment of the degree of internal carotid artery (ICA) diameter reduction. More recent reports reiterate the importance of stenosis in patients with transient ischaemic attacks (TIA) [(3, 4)]. The number of strokes prevented by expedited carotid endarterectomy (CEA) or carotid artery stenting (CAS) (within 14 days of symptom onset) is significantly greater in patients with 70–99% stenosis compared with those with 50–69% stenosis [(3, 4)].

The NASCET and ECST trials did not originally report similar outcomes, due in large part to each trial using a different method for measuring stenosis severity (outer edge versus diameter) [(5)]. A 70% stenosis calculated using the NASCET criteria, for example, corresponds to an 83% stenosis calculated using the ECST technique since the diameter of the distal ICA is smaller than the estimated outer edge of the ICA at the stenosis [Figure 1]. After a reanalysis of the ECST results using the NASCET method, the outcomes of the two studies were similar [(6)].

Figure 1 Grading of internal carotid artery stenosis - NASCET vs ECST criteria.

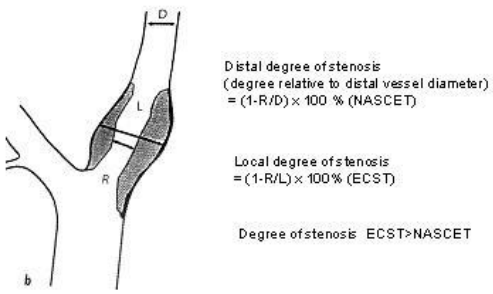

Distal (%)	0	50	60	67	70	75	85
Local (%)	40	70	75	80	82	85	90

The fundamental results achieved by the American and European trials have prompted an extensive worldwide effort to identify reliable and universally reproducible criteria to accurately grade ICA stenosis using Doppler ultrasound. The method relies mainly on velocity criteria and it has been used to provide national and international society consensus documents [(7-13)]. Several similarities can be found among the different consensuses, particularly a focal peak systolic velocity (PSV) >230 cm/s within the internal carotid artery stenosis and an internal carotid artery to common carotid artery (CCA) peak systolic velocity (ICA/CCA PSV) ratio >4, identify a ≥70% stenosis in symptomatic patients [(8, 9, 11, 13)].

Indications for ultrasound examination of the carotid arteries

The ultrasound detection and characterisation of severe carotid artery disease and preventive strategies like carotid endarterectomy can significantly reduce the incidence of stroke in at risk patients [(1, 7)]. However, it is not a cost effective strategy to screen asymptomatic patients in the community for carotid artery disease [(14)].

High risk patients are those with a history of stroke/transient ischaemic attack, neck bruits, peripheral arterial disease and coronary artery disease [(13)]. A duplex examination of the extracranial arteries should be mainly recommended in the following situations [(15)]:

- Patients with hemispheric neurological symptoms (i.e. stroke, transient ischaemic attack, amaurosis fugax).
- Evaluation of patients with cervical bruit.
- Patients with known coronary artery stenosis and/or peripheral arterial disease and/or proven carotid disease as per follow up.
- Asymptomatic patients ≥65 years old with cardiovascular risk factors (in particular hyperlipidaemia, arterial hypertension, diabetes mellitus, smoking).
- Patients scheduled for major cardiovascular surgical procedures (preoperative evaluation).
- Postoperative or post interventional patients after cerebrovascular revascularisation (e.g. carotid endarterectomy, stenting, etc.).
- Patients with symptoms of syncope or dizziness.
- Evaluation of pulsatile neck masses.
- Evaluation of non-hemispheric or unexplained neurological symptoms.

- Screening of high-risk patients, e.g. extra-carotid atherosclerosis, history of head and neck irradiation, known fibromuscular dysplasia (FMD), Takayasu arteritis or other extra-cranial vasculopathy.
- Neck trauma.
- Hollenhorst plaque (cholesterol embolus in retinal blood vessel) visualised on retinal examination.

Technical and methodological considerations

Ultrasound techniques can accurately depict arterial wall morphology using B-mode imaging and can simultaneously define carotid haemodynamics using colour Doppler flow and pulsed wave Doppler. Standard protocols should be used to ensure the reproducibility of the information collected [(16)].

The examination of extracranial vessels requires the use of B-mode and colour coded and/or power imaging with high frequency linear transducers. However, under particular circumstances such as in short and difficult necks, to investigate the very proximal or very distal carotid segments, to examine the vertebral arteries or in the presence of calcific arteries, lower frequency or curved array transducers may be necessary.

To detect a carotid stenosis, the highest peak systolic velocity is sought. The insonation angle should be ≤60°. The sample volume should be placed at and around the site of the narrowest region of an atherosclerotic lesion and can often be identified on colour Doppler flow as aliasing [Figure 2]. In addition to demonstrating elevated velocity at the site of the stenosis, colour Doppler detection of a poststenotic turbulence and a downstream demonstration of turbulence and/or 'tardus parvus' waveform [Figure 3 and 4] can further confirm and strengthen the diagnosis a significant (>70%) ICA stenosis.

Figure 2 B-mode and colour flow representation of a severe stenosis of the internal carotid artery with a focal increase in both PSV (326 cm/s) and end diastolic velocity (EDV) at the site of lumen reduction compared to the prestenotic values (a). The maximum lumen reduction and the colour velocity jet

(identified by aliasing) can be easily recognised and they can be used to place the sample volume of the spectral Doppler for velocity measurements (b).

a

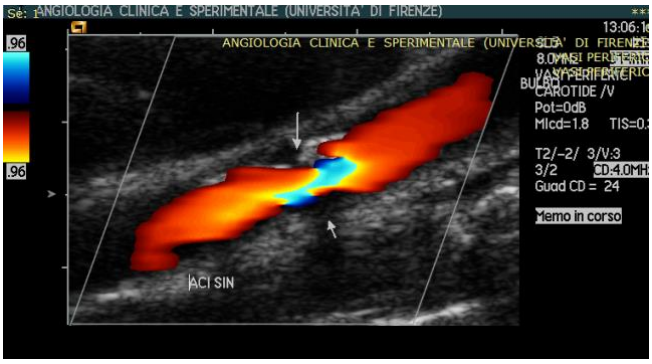

b

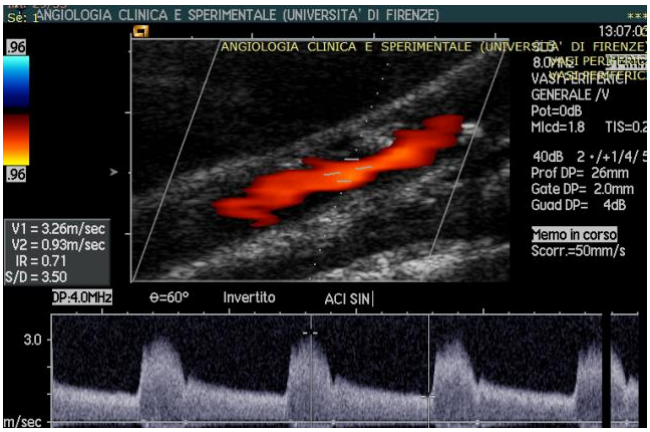

Figure 3 **Internal carotid artery stenosis with heterogeneous plaque and a 50-69% stenosis (a). On greyscale of the proximal ICA, there is irregular plaque which is hyperechoic, hypoechoic and anechoic. Plaque with anechoic spaces indicates heterogeneous plaque (b). Colour Doppler of the stenotic proximal ICA demonstrates aliasing associated with the narrowed segment. Distal to the stenosis there is widening of the artery with aliasing, red and blue indicating high velocity and simultaneous antegrade and retrograde flow (c). Spectral Doppler of the distal CCA before the bifurcation demonstrates a normal waveform. This velocity is used for the ICA:CCA ratio (d). ICA spectral Doppler before the stenosis demonstrates a normal waveform shape, no spectral broadening and a normal velocity (e). ICA spectral Doppler in the stenosis**

demonstrates elevated velocity of the stenotic jet. In the jet there is no spectral broadening since turbulence occurs after the stenosis. This is the site of maximal velocity and is used for velocity and for the IC velocity of the IC:CC ratio (f). ICA spectral Doppler just beyond the stenosis demonstrates the appearance of spectral broadening with filling in of the envelope and mild forward and reverse flow. The velocity is elevated but is lower than the maximal velocity at the jet (g). ICA spectral Doppler further distal to the stenosis demonstrates more severe spectral broadening with filling in of the envelope, poor definition of the peak velocity envelope and mild forward and reverse flow. The velocity is still elevated but lower than the maximal velocity at the jet (h). ICA spectral Doppler further distal from the stenosis shows a 'tardus parvus' waveform with lower velocity than the rest of the ICA.

a

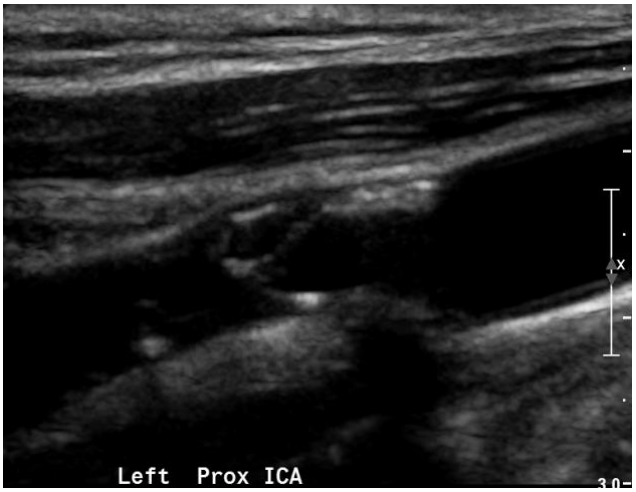

b

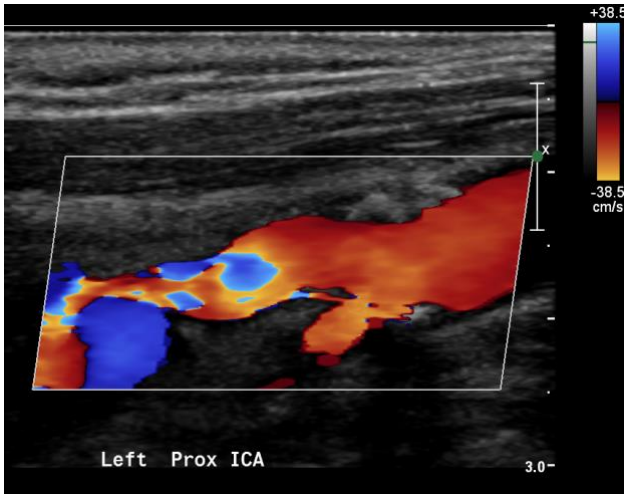

c

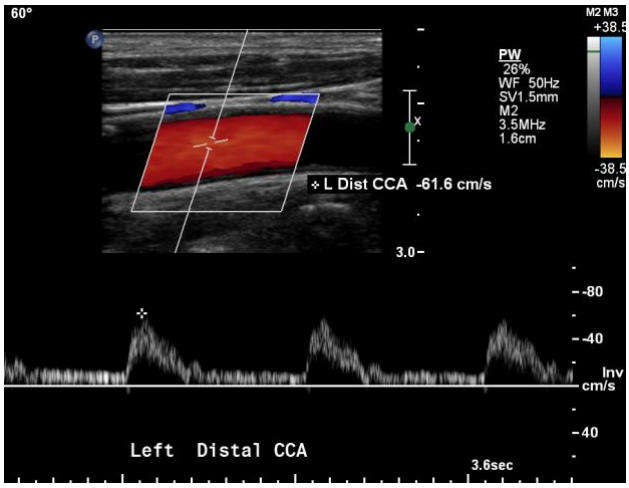
60°
M2 M3
+38.5
PW
26%
WF 50Hz
SV1.5mm
M2
3.5MHz
1.6cm
-38.5
cm/s
L Dist CCA -61.6 cm/s
3.0
-80
-40
Inv
cm/s
-40
Left Distal CCA
3.6sec

d

54°
M2 M3
+38.5
PW
34%
WF 50Hz
SV1.5mm
M2
3.5MHz
1.7cm
-38.5
cm/s
L Prox ICA -86.8 cm/s
3.5
-120
-80
-40
Inv
cm/s
Left Prox ICA

e

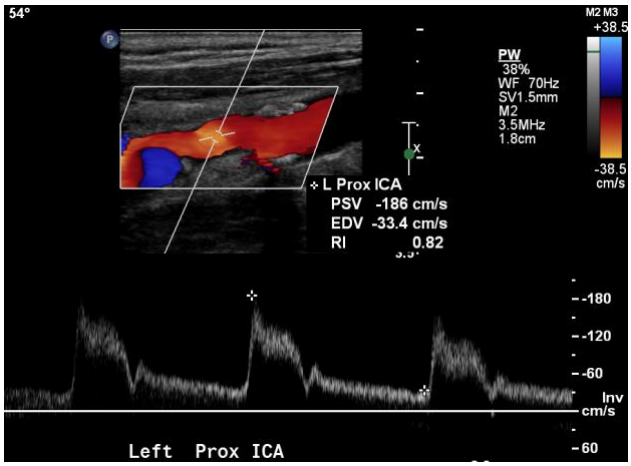
54°
M2 M3
+38.5
PW
38%
WF 70Hz
SV1.5mm
M2
3.5MHz
1.8cm
-38.5
cm/s
L Prox ICA
PSV -186 cm/s
EDV -33.4 cm/s
RI 0.82
-180
-120
-60
Inv
cm/s
-60
Left Prox ICA

f

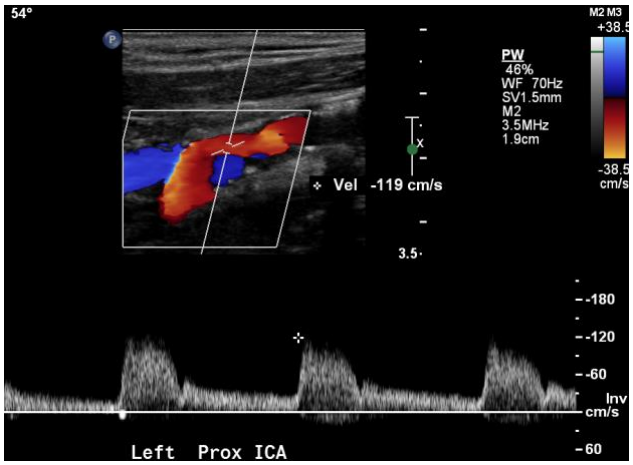

g

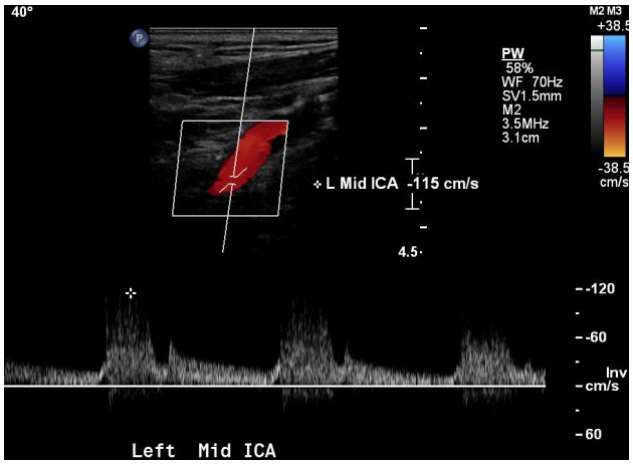

h

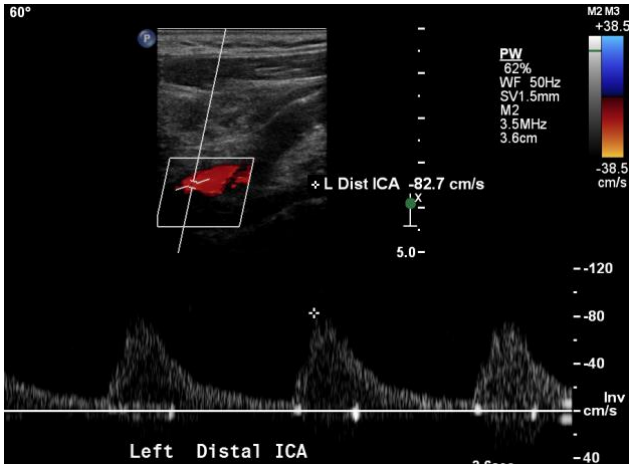

Figure 4 **Severe stenosis of the internal carotid artery using B-mode (a). Colour imaging of the stenosis shows an increase in velocity in the stenosis indicated by aliasing with dissipation of the jet distally and flow separation with reverse**

flow close to the artery wall (b). The spectral Doppler changes through the stenosis show normal peak velocity (PSV 58 cm/s) proximal to the stenosis (c) with an increase to 392 cm/s in the stenosis (d). Distal to the stenosis there is a jet in the centre of the artery (e). At the edge of the artery, reverse flow is observed (f). By opening up the sample volume to include the whole of the artery, the complex flow in the poststenotic region of the artery is demonstrated (g).

a

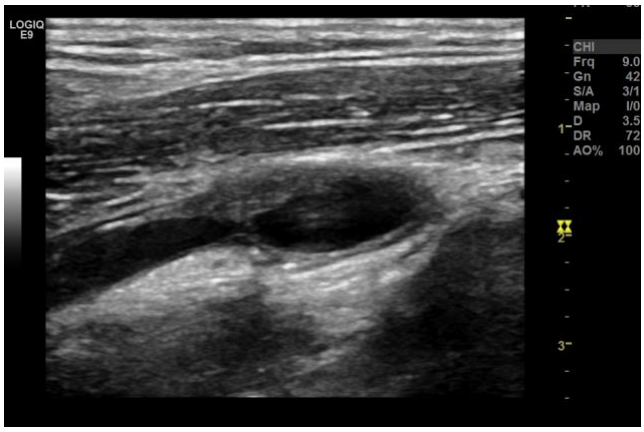

b

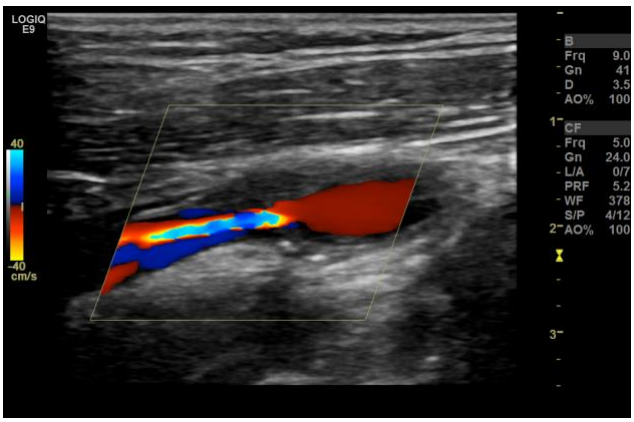

c

LOGIQ E9
PS 58.0 cm/s
ED 11.5 cm/s
INVERT
AC 60
cm/s

d

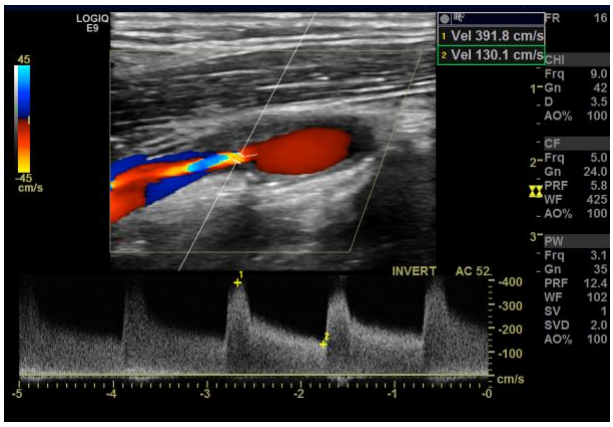
LOGIQ E9
Vel 391.8 cm/s
Vel 130.1 cm/s
INVERT
AC 52
cm/s

e

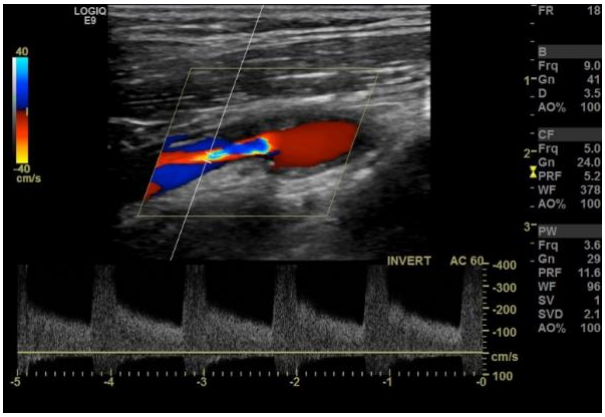
LOGIQ E9
INVERT
AC 60
cm/s

f

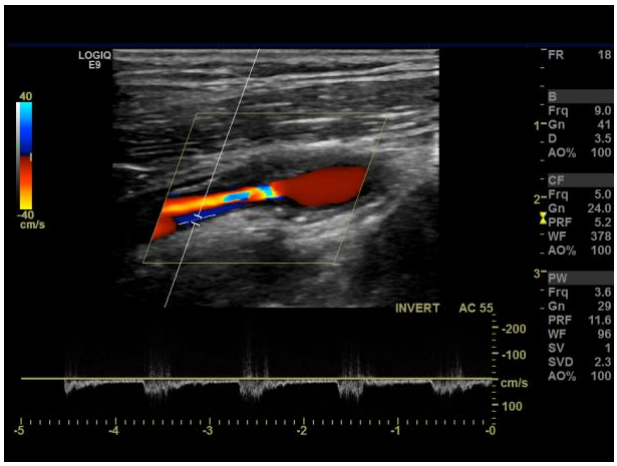

g

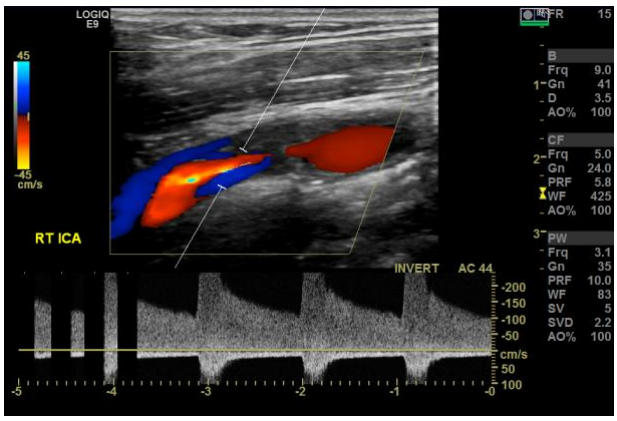

Early lesions and arterial wall characterisation: defining the thickness of the intima-media complex (IMT)

Ultrasound techniques allow measurement of the thickness of the arterial wall due to the appearance of the carotid arterial wall layers, namely the intima and media layers. The IMT is used to establish cardiovascular risk. Although the results of several studies indicate its value as an independent predictive risk factor of cardiovascular disease, to date [(17-19)] the presence of carotid plaque appears to be a more powerful predictor of cardiovascular risk compared to IMT alone [(20)]. Different protocols have been suggested, although a universal standard protocol has not been defined. The consensus meeting of the European Society of Neurosonology and Cerebral Hemodynamics held in Mannheim in 2004 recommends performing the IMT measurement in the distal and far wall of the common carotid artery, 1 cm away from the carotid bulb [(19)]. All measurements should be performed only if the

thickness of the arterial walls is homogeneous and devoid of atherosclerotic plaque (plaque does need to be commented upon). The normal IMT value in the general population is ≤0.9 mm; this value must be assumed as a cut-off limit regardless of age, although the upper limit can slightly vary according to age, gender and race [(21)]. The evaluation of the IMT can be done free-hand on the basis of the average value of at least three adjacent measurements. Alternatively a semi-automatic estimate can also be performed through dedicated software that can provide a single measurement derived from the average value of many measurements in a 1 cm segment [Figure 5].

Figure 5 Semi-automatic intima-media thickness (IMT) measurement. A computer assisted 'edge' tracking software allows an operator-independent estimate of the average thickness of the IMT complex along a 1 cm segment of the far wall of the distal common carotid artery.

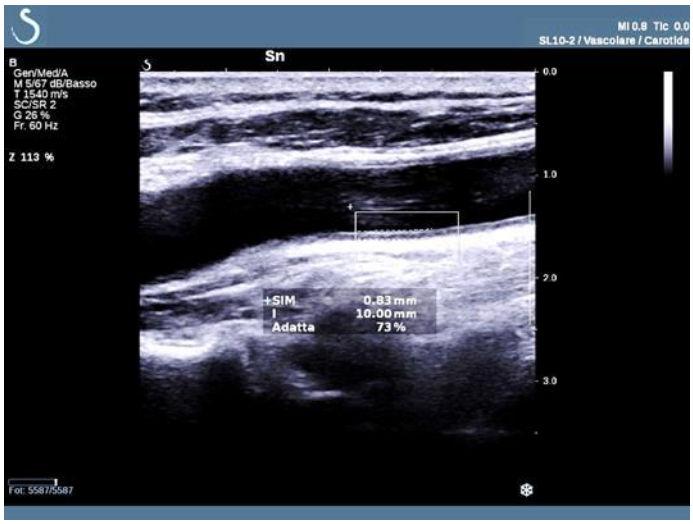

Atherosclerotic plaque

An atherosclerotic plaque is defined as a ≥1.5 mm focal thickening of the arterial wall protruding into the arterial lumen or a focal thickening exceeding the thickness of the adjacent unaffected arterial segment by more than 50% [(19)]. The 'histological' characterisation of an atherosclerotic plaque can be performed using ultrasound, however

its accuracy and reproducibility is operator dependent. Some studies have found poor correlation or no correlation at all between sonographic and histological findings [(22-24)] but ultrasound features of atherosclerotic plaques can correlate with patient symptoms [(25)]. It has also been shown that excellent results can be obtained with visual plaque assessment with proper attention to imaging details [(26)]. As suggested by De Bray et al [(27)], satisfactory and fairly reproducible results can be achieved by comparing the plaque echogenicity with the one found in the following reference structures: a hypoechoic plaque corresponds to the echogenicity of flowing blood, an intermediate echogenicity to that of the sternocleidomastoid muscle and an hyperechoic plaque to that of bony structures. The 'eye-ball' morphological characterisation by ultrasound techniques allows different plaques to be distinguished according to echogenicity, homogeneity (homogeneous vs hetereogeneous) and their surface (regular, irregular or ulcerated plaques). In adherence with such criteria, 5 different classes of atherosclerotic plaques have been proposed by Gray-Weale and colleagues [(28)] and by Geroulakos and coworkers [(29)]. The table shows the risk level associated with each plaque category [Table 1]**.**

In order to overcome the problem of inter-operator variability, some more reproducible techniques have recently been introduced. These include videodensitometry and radiofrequency analysis. In the ICAROS (Imaging in Carotid Angioplasty and Risk of Stroke) study, for example, a greyscale median analysis of plaques measured by a computer assisted technique, has been proven to be effective in identifying echolucent vulnerable plaques in patients undergoing carotid stenting [(30)]. Intravascular ultrasound computerised texture analysis of symptomatic carotid plaques has also been used to identify those that are associated with brain infarction [(31)].

At B-mode examination the plaque surface can be very irregular with excavations. The finding of a $\geq$2 mm deep excavation is consistent with an ulcerated plaque [Table 6]. To avoid misinterpretation due to serial plaques, the presence of an ulcer should always be confirmed in both longitudinal and transverse scanning planes.

Table 1 Carotid plaque classification (slightly modified) according to Gray-Weale and the relative grade of risk.

CAROTID PLAQUE TYPES	RISK OF SYMPTOMS

Type 1: Uniformly hypoechoic (echolucent)	High
Type 2: Predominantly hypoechoic (echolucent) (>50% of plaque structure)	High
Type 3: Predominantly echogenic (>50% of plaque structure)	Lower than type 1 and 2
Type 4: Uniformly echogenic	Lowest
Type 5: Unclassified due to calcification or poor visualisation	Unknown

Figure 6 Representations of surface irregularities (a) and an ulcerated plaque (b) as confirmed by CTA (c).

a

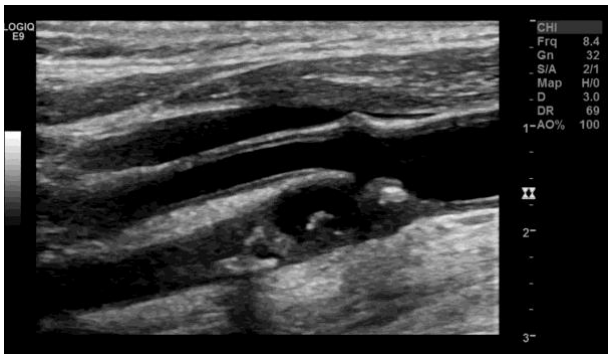

b

c

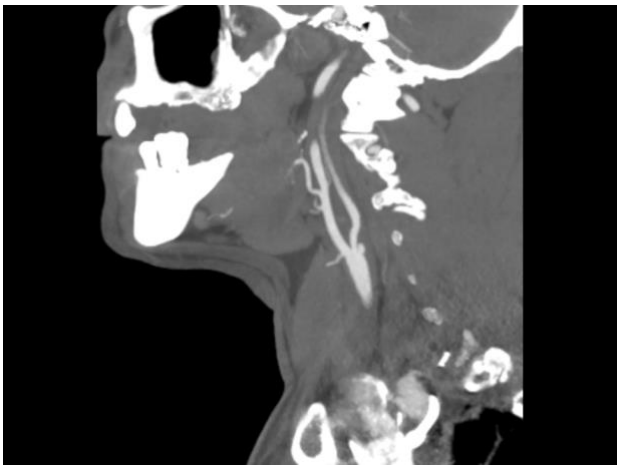

Some additional parameters of plaque instability have been more recently described, particularly neovascularisation. It has been demonstrated that plaque neovessels can be effectively detected by colour and power flow imaging. These preliminary reports in studies with small sample sizes have found a positive correlation between sonographic and histological findings. In addition, the presence and number of neovessels showed a correlation between embolic activity [Figure 7] and the histological signs of inflammation [(32, 33)]. Technological progress such as contrast enhanced ultrasound (CEUS) [(34)] are also encouraging. A recent retrospective study on 147 stroke patients undergoing CEUS has reported that the presence and degree of adventitial neovessels (vasa vasorum) and plaque neovascularisation were associated with cardiovascular deaths and cardiovascular events [(34)]. However the method still needs to be standardised and the data will need to be confirmed by larger trials.

Figure 7 Carotid artery stenosis. Contrast enhanced ultrasound indicates multiple sites of neovascularization (a). B flow imaging can also provide a direct evidence of the presence and number of microvessels. The bright spots within the plaques indicate multiple sites of vascularization (b). In a 79 years old patient with recent ischemic stroke, carotid stenosis and transcranial Doppler evidence of ipsilateral microembolic signals (HITS). The B flow study showed extensive carotid plaque vascularization (c).

a

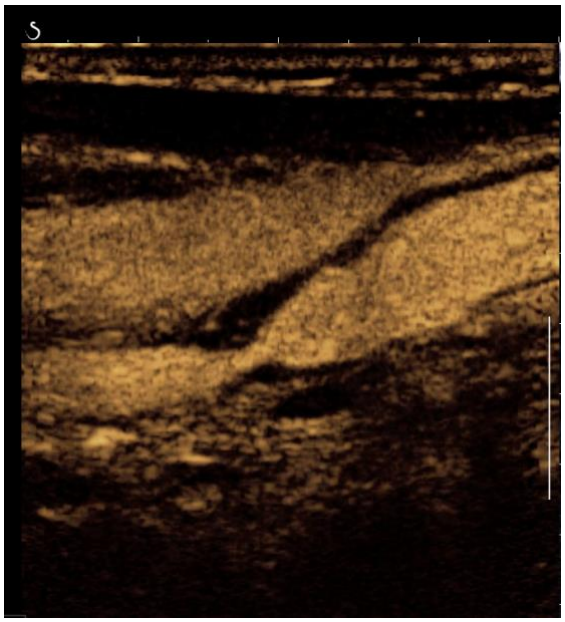

b

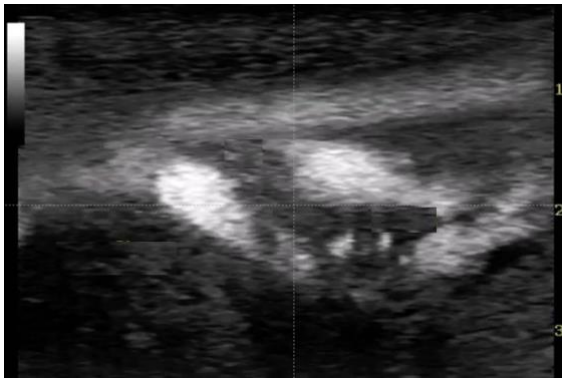

c

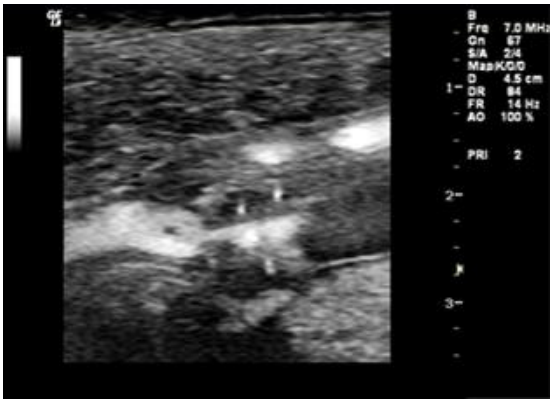

3D ultrasound may be another technique used to define the atherosclerotic burden of a whole section of a carotid artery [Figure 8]. Despite the potential benefit, the technique is not yet widely available.

Figure 8 3D imaging of the common carotid artery. The longitudinal and cross sectional views can accurately define the global atherosclerotic burden of the vessel.

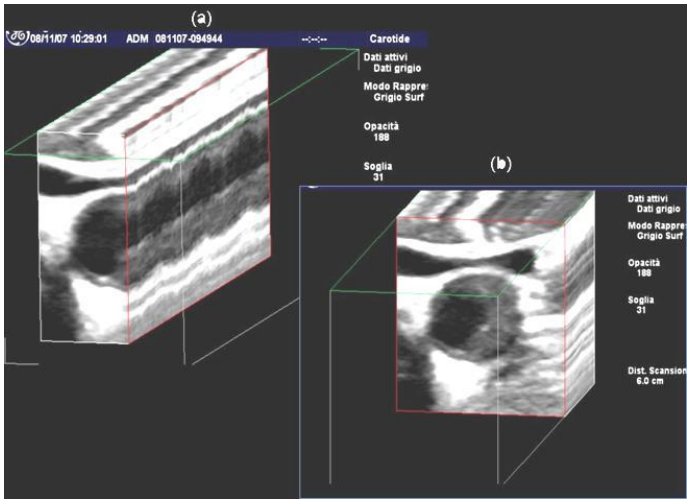

Protocol

Colour Doppler flow and pulsed wave Doppler allow assessment of the haemodynamic function of the carotid and vertebral arteries. The B-mode imaging analysis must be routinely performed using both the transverse and longitudinal planes by applying the transducer posteriorly or anteriorly, along the sternocleidomastoid muscle [Figure 9].

Figure 9 2D longitudinal and transverse views of the middle part of the common carotid artery (CCA, a, b) and carotid bifurcation (c, d). IJV: Internal jugular vein. ECA: External carotid artery.

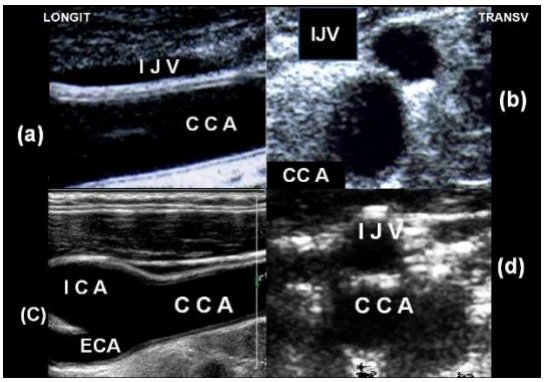

B-mode imaging, combined with colour Doppler flow provides a roadmap for accurate spectral Doppler haemodynamic testing of specific sites of interest on the longitudinal sections. Complications, such as arterial dissection can be diagnosed [Figure 10].

Figure 10 An abrupt and remarkable ICA narrowing ('pig-tail' appearance) is the hallmark of the fibrous scarring remodelling of an acute, dissected carotid artery. The extreme vessel tapering can cause extensive stenosis reflected by colour Doppler turbulent flow (a), a focal increase in PSV (b) and is anatomically well defined by power imaging (c,d).

a

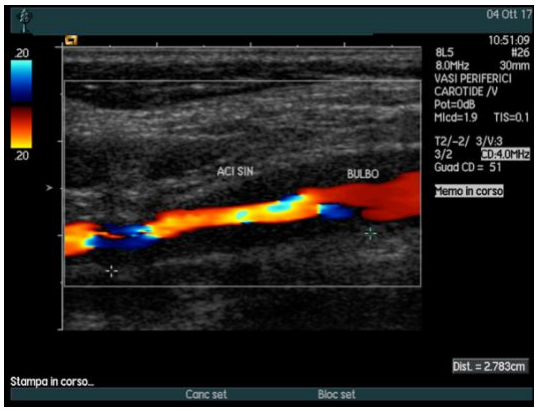

b

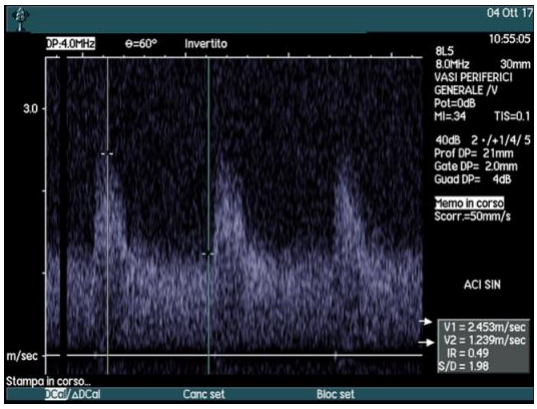

c

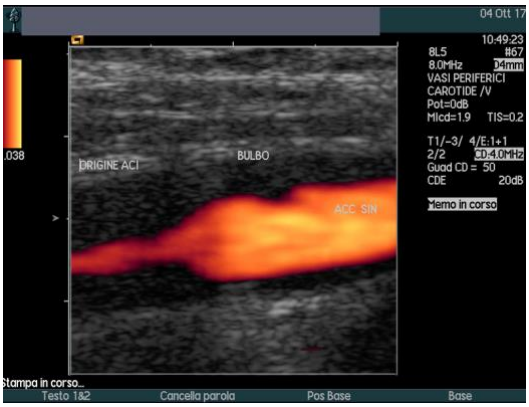

d

Pulsed wave Doppler examination should be performed on the common, external and internal carotid arteries; each artery has a typical spectral Doppler waveform. The diastolic portion of the waveform is generally related to the downstream vascular bed; the brain is a low resistance territory, therefore the Doppler waveform of vessels feeding the brain will show more pronounced diastole, while those vessels feeding a high resistance territory such as the face and the thyroid will have a smaller amount of diastolic flow. Therefore, the

vessels supplying the brain (internal carotid artery and vertebral arteries) show a rapid upstroke with a low-resistance Doppler waveform profile with forward flow throughout the cardiac cycle. ICA diastolic velocity is typically 1/3 to 1/2 of the systolic velocity. The external carotid artery (ECA) is more pulsatile than the ICA and shows a high resistance Doppler waveform; the ECA Doppler waveform exhibits a deep diastolic notch perhaps with early diastolic reverse; the CCA profile is usually somewhat intermediate as it reflects elements of the ICA and ECA patterns [Figure 11].

Figure 11 Schematic representation of the low and high resistance and intermediate velocity profiles typically observed in the internal (ICA), external (ECA) and common carotid arteries.

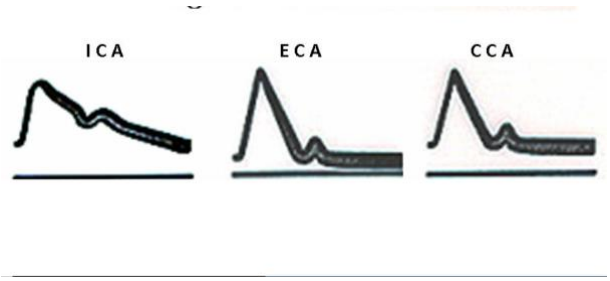

Another technique to distinguish the ICA from the ECA is the tapping manoeuvre. By tapping with a finger over the superficial temporal artery in front of the ear, saw-tooth alterations of the diastolic phase can be noted on the pulsed wave Doppler ECA waveform. This is not generally seen on the ICA Doppler waveform [Figure 10]. Since temporal tapping has not been found to be reliable in a small minority of subjects, the ECA should be identified by additional criteria such as identifying its branches, smaller size and typical waveform.

Figure 12 Typical saw-tooth appearance of the velocity profile of the external carotid artery during the so called 'tapping' manoeuvre. No signal modulation can be detected in the internal carotid artery during oscillating temporal compression.

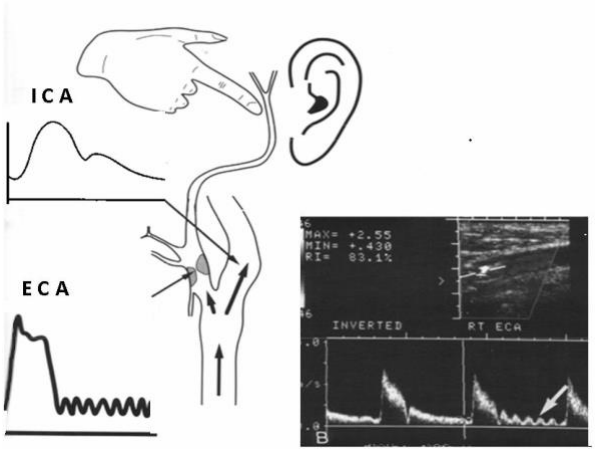

Grading the carotid stenosis

The estimate of the degree of stenosis by direct measurement of the minimum viable lumen diameter or through its planimetric evaluation is usually accurate for stenosis <50%. Calcification may obscure the lumen even in minor disease. For ≥50% stenoses, Doppler velocity estimates are more accurate and are the method of choice. The diagnosis of carotid stenosis by spectral Doppler is made by the demonstration of a focal velocity elevation at the level of the lumen reduction and lower velocity and turbulence downstream. The first demonstration of a direct and positive relation between a focal flow velocity and the degree of diameter reduction of the internal carotid artery was provided by Spencer [(35)] [Figure 13]. A meta-analysis of 41 studies performed by Wardlow including 4876 carotid arteries in 2541 patients has demonstrated that Doppler velocity measurements and neuroradiological measurements give similar results in carotid stenoses ranging from 70 to 99% diameter reductions [(36)].

Figure 13 Flow velocity and volume flow in the carotid artery at increasing values of diameter reductions. Initially, velocity increases in inverse proportion to the

decrease in area. As the stenosis severity increases, flow is reduced. Velocity continues to rise but reaches a peak and falls in very severe stenosis.

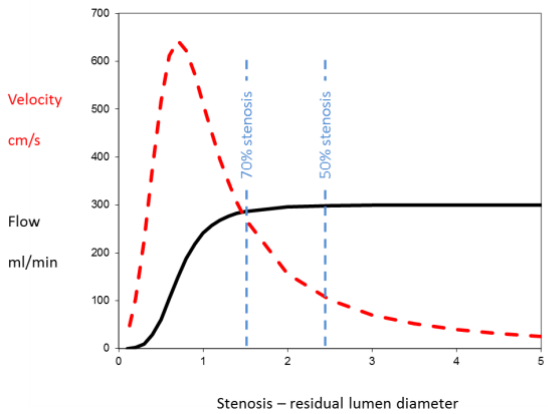

The increase in velocity is proportional to the severity of the stenosis and it is highest in 80-99% stenosis. At near to occlusion conditions (>99% stenosis), the high friction, elevated resistance to flow and the dominance of collateral supply to the cerebral circulation leads to a drop in flow velocity. The spectral Doppler protocol consists of profiling the stenosis with recordings proximal to the stenosis (typically the CCA), at the point of maximal velocity and distal the stenosis. Scanning while moving the sample volume around site of maximum lumen reduction (by greyscale and colour flow) is performed to detect the maximal velocity [Figure 2]. Scanning beyond the stenosis is also performed and a poststenotic sample recorded. A stenosis should have the angle corrected peak systolic velocity higher than the cut-off value for the stenosis grade and should also demonstrate lower velocity (typically spectrally broadened flow) beyond the jet that is due to turbulence. A >50% stenosis is assumed at peak systolic flow velocities >125 cm/s and a 70-79% stenosis at >230 cm/s. The sensitivity and specificity of such velocity criteria are 90-96% and 86-93% respectively, according to several studies [(37-39)]. Angiographic evaluation has shown a good correlation between mean PSV and percentage of stenosis as measured arteriographically [(40)].

Different systemic conditions may lead to elevated peak systolic velocity throughout the entire circulation. The internal carotid artery to common carotid artery velocity ratio (Vmax ICA/Vmax CCA ratio) can effectively diagnose and grade carotid stenosis severity in the face of diffuse velocity increases. The ICA/CCA ratio varies between 2 and 4 in cases of 50-70% stenosis [(8, 9, 11, 13)] and is greater than 4 in cases of 70-99% stenosis [(8, 9, 11, 13)].

Most operators use the ICA PSV unless CCA velocities are elevated (typically more than 100 cm/s). In those instances the ICA/CCA ratio is preferred. Diastolic velocity or elevated ratios can be used for greater degrees (70–99%) of stenosis [(41, 42)] [Figure 14].

Figure 14 Color flow settings show a high velocity jet with local aliasing suggesting a stenosis (a). The ICA stenosis and its longitudinal extension can be also visualized by directional power Doppler imaging (b). At the point of color flow aliasing, PSV exceed 336 cm/s and EDV exceed 130cm/s consistent with a 80-95% stenosis (c).

a

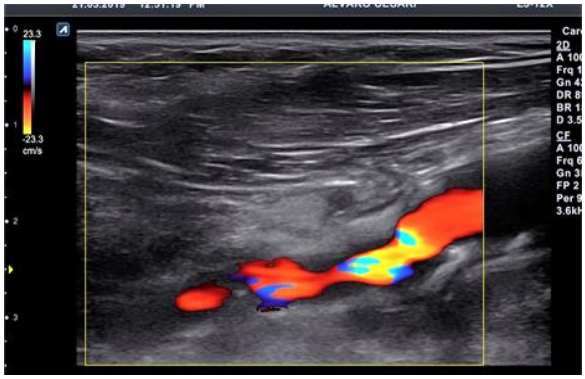

b

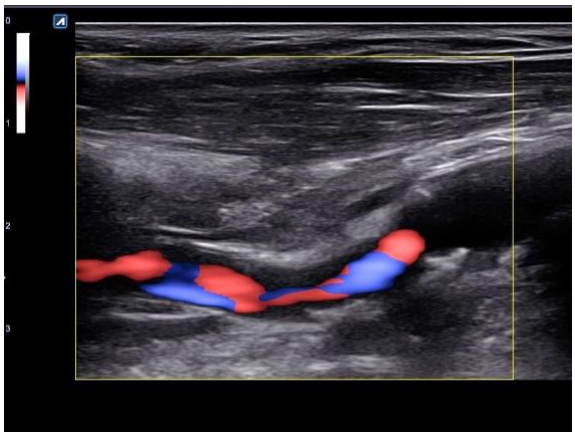

c

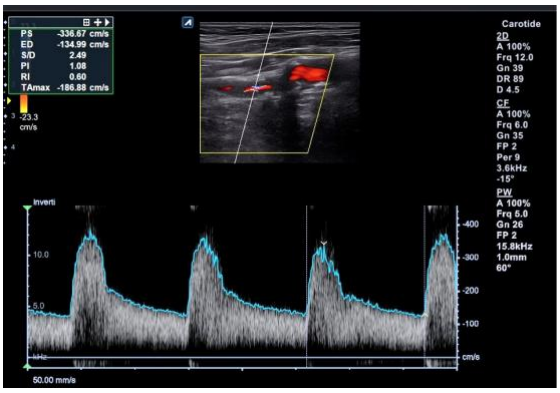

Diastole may be more specific since greater degrees of stenosis have better pressure reduction through the entire cardiac cycle [(41, 42)]. Some groups recommend combinations of parameters (Table 4] [(10)]. While multiple parameters may lead to a more reliable grading of stenosis, the exact rules to combine parameters are not universally accepted. In addition, a recent investigation tested the agreement between Duplex ultrasound (DUS) and CT angiography using a multiparametric approach and DUS revealed several differences between the two modalities [(43)].

Grades of less than 50%, 50-69%, >70% to less than near occlusion, near occlusion and occlusion have been recommended as the grades to be reported [(12)] [Figure 15].

Figure 15 Suspected total stenosis by conventional Doppler techniques (a,b). 'Near occlusion' could be proven by contrast enhanced ultrasound (CEUS), a much more sensitive method compared to Doppler (c). Note the small jet next to the wall (b) (EFSUMB cases of the month, www.efsumb.org).

a

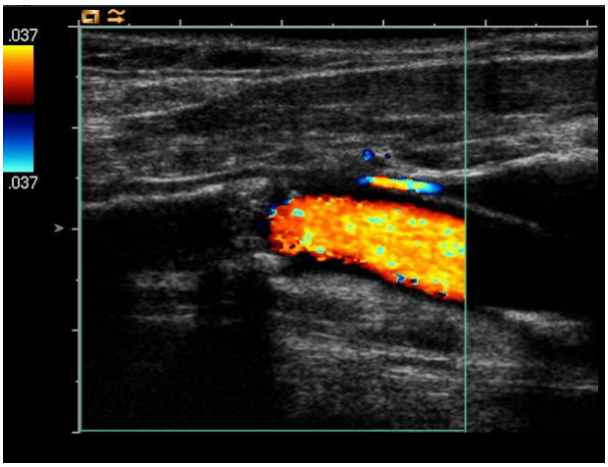

b

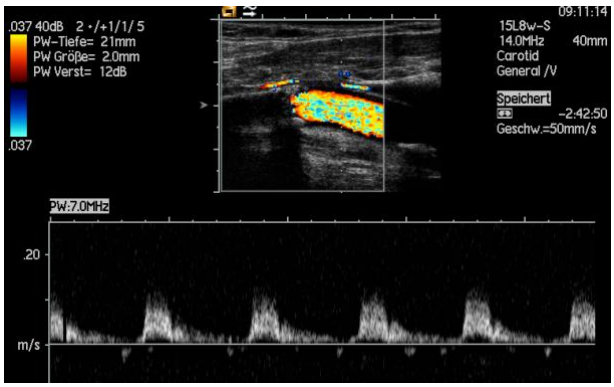

c

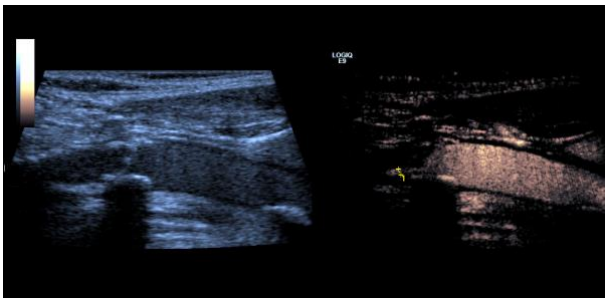

Moneta et al [(44)] found that an ICA/CCA PSV ratio of >4 was associated with a >70% stenosis when measured according to the NASCET method, with a sensitivity of 0.91 and a specificity of 0.87. Grant et al. [(38)] found in their series that only 80% of all stenoses were correctly classified as >70% by an ICA/CCA PSV ratio >4. Other grades, particularly for evaluating higher degrees of stenosis prior to stenting, have also been proposed. The velocity criteria adopted in different vascular laboratories and reported in the literature are often different. Therefore, vascular laboratories should apply their own velocity criteria only

if they have been developed and validated through angiographic correlation in a large number of patients, otherwise, consensus or society recommendations should be adopted [Tables 2-4].

Table 2 B-mode and Doppler ultrasound criteria for the diagnosis of ICA stenosis.

Degree of Stenosis (%)	Primary Parameters		Additional Parameters	
	ICA PSV (cm/s)	Plaque Estimate (%)*	ICA/CCA PSV Ratio	ICA EDV (cm/s)
Normal	<125	None	<2.0	<40
<50	<125	<50	<2.0	<40
50-69	125-230	≥50	2.0-4.0	40-100
≥70 but less than near occlusion	>230	≥50	>4.0	>100
Near occlusion	High, low or undetectable	Visible	Variable	Variable
Total occlusion	Undetectable	Visible, no detectable lumen	Not applicable	Not applicable

Table 3 Recommendations for reporting carotid ultrasound investigations.

Percentage stenosis (NASCET)	Internal carotid peak systolic velocity cm/s	Peak systolic velocity ratio ICA_{PSV}/CCA_{PSV}	St Mary´s ratio ICA_{PSV}/CCA_{PSV}
<50	<125[a]	<2[a]	<8
50-59	>125[a]	2-4[a]	8-10
60-69			11-13
70-79	>230[a]	>4[a]	14-21
80-89			22-29
>90 but less than near occlusion	>400[b]	>5[b]	>30
Near occlusion	High, low – string flow	Variable	Variable
Occlusion	No flow	Not applicable	Not applicable

Table 4 Combined criteria for grading internal carotid stenosis.

Degree of stenosis as defined by NASCET (%)	Grading of internal carotid stenosis						
	10-40	50	60	70	80	90	Occlusion
Main criteria							
1. B-mode image, diameter	Applicable	Possibly applicable					Imaging of occluded artery
2. Colour doppler image	Plaque delineation	Flow	Flow	Flow	Flow	Flow	Absence of flow
3. PSV threshold (cm/s)		125		230		NA	NA
4.. PSV average (cm/s)	≤160	210	240	330	370	Variable	NA
5. Collateral flow (periorbital arteries or circle of Willis)				Possible	Present	Present	Present
6. Prestenotic flow (diastole) (CCA)				Possibly reduced	Reduced	Reduced	Reduced
7. Poststenotic flow disturbances (severity and length)		Moderate	Pronounced	Pronounced	Pronounced	Variable	NA
8. End-diastolic flow velocity in the stenosis (cm/s)			<100	>100		Variable	NA
9. Carotid ratio ICA/CCA	<2	≥2	≥2	>4	>4	Variable	NA

These criteria do not apply for external carotid stenosis. Note the hierarchical order of main and additional criteria and the change of reliability of each criterion.

Table 5 Combined criteria for grading internal carotid artery stenosis.

Degree of stenosis as defined by NASCET (%)	Grading of internal carotid stenosis						
	10-40	50	60	70	80	90	Occlusion
Main criteria							
1. B-mode image, diameter	Applicable	Possibly applicable					Imaging of occluded artery
2. Colour Doppler Image	Plaque delineation	Flow	Flow	Flow	Flow	Flow	Absence of Flow
3. PSV threshold (cm/s)		125		230		NA	NA
4a. PSV average (cm/s)	≤160	210	240	330	370	Variable	NA
4b. PSV poststenotic (cm/s)				≥50	<50	<30	NA
5. Collateral flow (periorbital arteries or circle of Willis)				Possible	Present	Present	Present
Additional criteria							
6. Prestenotic flow (diastole) (CCA)				Possibly reduced	Reduced	Reduced	Reduced
7. Poststenotic flow disturbances (severity and length)		Moderate	Pronounced	Pronounced	Pronounced	Variable	NA
8. End-diastolic flow velocity in the stenosis (cm/s)			<100	>100		Variable	NA
9. Carotid ratio ICA/CCA	<2	≥2	≥2	>4	>4	Variable	NA

These criteria do not apply for external carotid stenosis. Note the hierarchical order of main and additional criteria and the change of reliability of each criterion.

Other vessels

Direct quantification of a significant (>50%) stenosis of the brachiocephalic trunk or of the left proximal common carotid artery may be difficult due to limited imaging and views of these segments. However, severe disease in these vessels should be always suspected if the cervical CCA waveform shows unusual flow ('tardus parvus' or 'steal-type') waveforms. Diagnosis may require CTA or MRA. A diagnostic problem may be encountered if obstructive disease involves the distal or intracranial internal carotid artery, inaccessible to the routine extracranial carotid examination. Focal velocity increases at the level of the obstruction are not directly visible but the finding of a low systolic peak velocity or high pulsatility in the ICA should prompt further examination for distal disease by CTA or MRA imaging.

Vertebral Arteries

Introduction

The vertebrobasilar system is responsible for 20 to 30% of intracranial blood flow. Although ischaemic stroke in the vertebrobasilar system is less common than in the carotid system, abnormal Doppler and Duplex examinations are at least as frequent in the vertebrobasilar system as in the carotid system [(45)].

Vertigo is the most common symptom of vertebrobasilar insufficiency (VBI). It is abrupt in onset and it is most commonly associated with other typical signs and symptoms such as ataxia, drop attacks, blurred or double vision, nausea and vomiting. Given its usual presentation, the clustering of clinical symptoms observed in patients with vertebrobasilar insufficiency can readily direct the workup towards a posterior circulation defect and an ultrasound to rule out vertebrobasilar disease. The distinction between ischaemia of the labyrinth and that of the brainstem or of both structures may not be so straightforward based on clinical grounds as the blood supply to the labyrinth, eighth cranial nerve and vestibular nuclei all originate from the same source, i.e. the vertebrobasilar circulation. In a few patients, a VBI dependent vertigo can occur as an isolated symptom [(46, 47)]. In these cases, the clinical diagnosis may be initially challenging since the dizziness may also be attributed to different causes such as acute myocardial infarction or dehydration. In some cases, a VBI dependent vertigo should be suspected when dizziness typically recurs after

sustained exercise of the arm ipsilateral to a subclavian steal. Apart from atherosclerotic lesions, acute symptoms of vertebrobasilar insufficiency may be due to dissection, typically occurring after trauma.

There are no strict and specific indications for the systematic ultrasound evaluation of the vertebrobasilar system but it is indicated for clinical suspicion of recurrent ischaemia in the vertebrobasilar artery territory and for patients with significant side to side differences in brachial blood pressures. The findings of vertebrobasilar obstruction do not always explain non-specific symptoms. Moreover, significant obstruction of a subclavian or vertebral artery may often be asymptomatic due to intra or extracranial collateral mechanisms.

Anatomy

The two vertebral arteries originate from the ipsilateral subclavian arteries at the level of the 6th cervical vertebra (V0). In 4% of all subjects the left vertebral artery originates directly from the aortic arch [(45, 48)]. The prevertebral section of the vertebral artery (V1) is defined as spanning from the subclavian artery to where it enters the spine through the costotransverse foramina at the 6th vertebrae. Both vertebral arteries proceed cephalad in the posterior aspect of the neck through the transverse foramina of the corresponding vertebrae (V2). The following part of the vertebral arteries courses superiorly and winds around the atlas, at the side of the medulla oblongata and at the level of the atlanto-occipital interspace. This segment is therefore also referred to as the atlas loop (V3). Muscular branches arising from the V3 segment form anastomoses with the occipital artery, a branch of the external carotid artery [(45)]. Finally the vertebral arteries proceed cephalad and anteriorly until they reach the pontomedullary level, where they join to form the basilar artery (V4) [Figure 16].

Figure 16 Anatomical representation of the different segments of the vertebral artery. V0 - at the origin from the subclavian artery. V1 - from the origin to the site of entry into the transverse foramen of the 6th cervical vertebra. V2 - the cervical intraforaminal segment. V3 - the upper segment winding around the atlas (atlas loop). V4 - the terminal intracranial segment joining the contralateral vertebral artery to form the basilar artery.

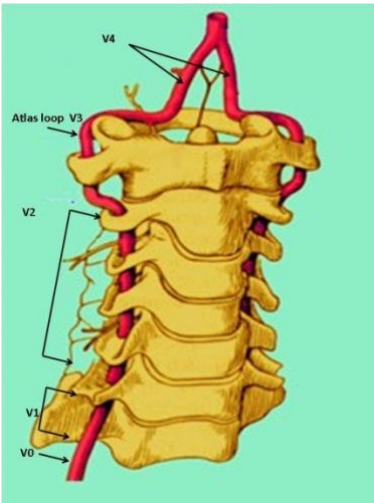

Branches of the basilar artery supply the entire pons and the superior and anterior aspects of the cerebellum. Branches of the vertebral arteries supply the medulla and the interior surface of the cerebellum [(49)]. Lack of symptoms, even in the presence of severe stenosis or occlusion of a subclavian or proximal vertebral artery, is often due to the presence and efficiency of a thyrocervical collateral vessel arising from the ipsilateral external carotid artery [Figure 17]. In a small number of patients, one of the vertebral arteries may terminate into the posterior inferior cerebellar artery instead of joining the contralateral vertebral artery. In a few subjects one vertebral artery can exclusively supply a muscular compartment of the neck.

One vertebral artery may be hypoplastic. This results in a high resistance pattern on spectral Doppler examination and may be misleading since low diastolic flow may be interpreted as the consequence of a distal obstruction rather than a benign anatomical variant.

Figure 17 Schematic representation of a thyrocervical collateral artery from the external carotid artery due to obstruction of the ipsilateral subclavian artery or the proximal vertebral artery.

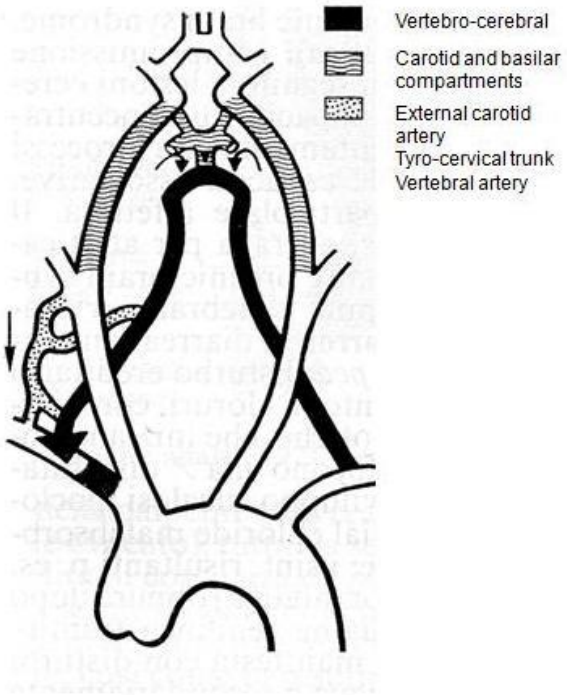

Ultrasound aspects

Proximal segments (V0-V1)

The V0 and V1 segments of the vertebral artery course behind and underneath the clavicle and therefore their visualisation is not always achieved. The examination of the proximal segment may be attempted if there are abnormal V2 waveforms. The prevertebral segment is the most common site of stenosis; virtually all stenoses of the vertebral artery occur at its origin [(49)]. The origin of the vertebral arteries and their proximal intrathoracic segment (V0 and V1) can be visualised by placing the probe at the level of the supraclavicular fossa [Figure 18].

Figure 18 The origin of the vertebral artery (V0) from the subclavian artery can be studied with a supraclavicular approach. The colour and power angio images show the proximal part of the left subclavian giving rise to the vertebral artery.

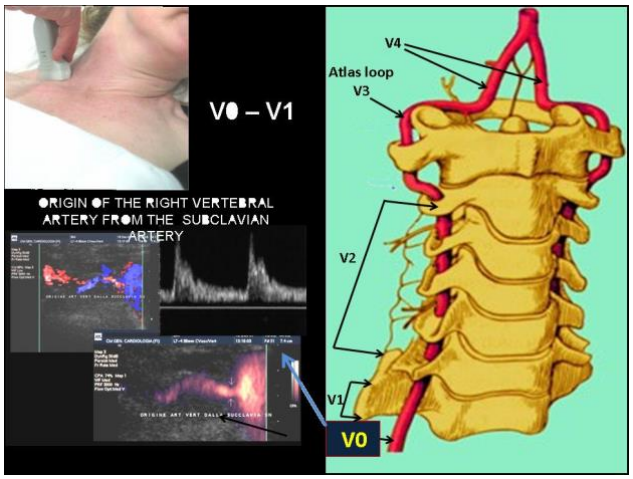

The origin can also be often difficult to image due to tortuosity and size variations (especially congenital hypoplasia). The origin and proximal segment of the vertebral artery may be confused with other large branches arising from the proximal subclavian artery, such as the thyrocervical trunk. The vertebral artery and vessels likely to be mistaken for the vertebral artery may be distinguished from each other by scanning the area in the supraclavicular fossa and performing an oscillation manoeuvre.

Compression of the V3 segment (between the tip of the mastoid and the transverse process of the atlas) allows the distinction between the vertebral artery and other vessels. The compression leads to unmistakable signal modulation of the V0 vertebral waveform assuming a typical saw-tooth appearance. The detection of a turbulent flow at the V0 to V2 level is indicative of a significant stenosis. Focal increases in velocity values may also be diagnostic. The peak velocity is usually compared with the velocity in more distal segments (>50% difference indicates a stenosis). A high grade stenosis may also be identified on the basis of a focal increase in peak systolic velocity of ≥150 cm/s [(50)].

V2 segment

The more reliable approach to assess the vertebral arteries is to begin the examination by scanning the vessel in longitudinal plane near its mid-segment (region V2). This segment is

more easily visualised, its course is typically straight and it does not usually exhibit any tapering or diameter changes. In addition, it is rarely affected by atherosclerotic lesions. It is possible to obtain adequate imaging and quantitative pulsed wave Doppler velocity data from some portions of the mid segment of the extracranial vertebral arteries in more than 98% of patients and vessels [(50)]. The examination is most easily accomplished by first obtaining a good longitudinal view of the common carotid artery at the approximate level of the third to fifth cervical vertebrae. Once this image has been obtained, angulating the probe laterally and inferiorly will bring the vertebral artery into view. The colour Doppler imaging identifies the artery flow by its pulsatile pattern of colour flow interrupted by a series of anechoic bands from shadowing by the transverse processes of the cervical spine [Figure 19].

Figure 19 The figure shows how to scan cervical region to explore the V2 segment of the vertebral artery. Apply the transducer longitudinally anteriorly, along the sternocleidomastoid muscle. Angulate the probe parallel to the carotid artery, laterally and inferiorly. Look for vertebral bodies: arcuate hyperechoic echoes which shadow. The flow velocity profile in the normal vertebral artery has a typically low resistance pattern.

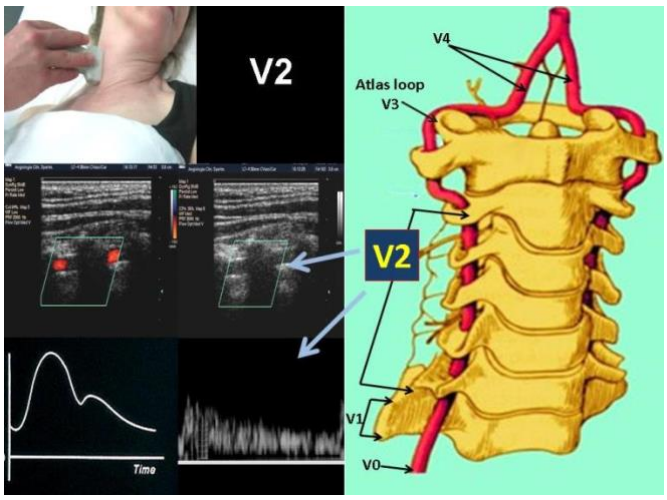

V3 segment (atlas loop)

In order to examine this segment the patient is asked to turn their head and the transducer is placed in a transverse position on the posterior aspect of the neck under the mastoid prominence [Figure 20]. Segment detection rates of 76% on the right and 86% on the left have been reported [(51)]. The B-mode examination alone mostly fails to detect the segment but colour Doppler eases its identification. The V3 segment is typically 'comma-shaped' [Figure 20]. The rounded course of the vessel does not allow an appropriate angle correction for velocity measurements. No systematic values have been reported; the velocity data collected in the V2 segment may be used [(51)].

Figure 20 Typical 'comma' appearance of the V3 segment at colour Doppler examination with characteristic profiles of spectral Doppler.

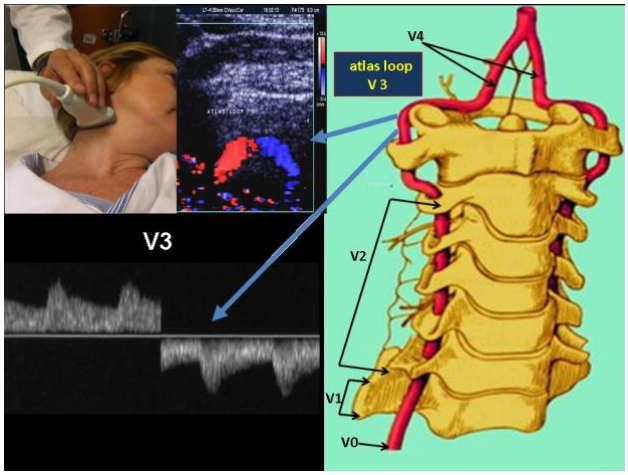

V4 (intracranial) segment

The confluence of the distal part of the vertebral arteries giving origin to the basilar artery can be examined by transcranial colour coded sonography (TCCS) using a low frequency (2.5-3.5 MHz) sector probe through the posterior suboccipital approach. The vertebral artery and the origin of the basilar artery are examined by placing the probe over the midline in the space between the occipital bone and the atlas, with the patient in a supine position with their head rotated laterally by 30 to 45° [(45)]. The foramen magnum and the hyperechoic

clivus serve as the anatomical landmarks, with both vertebral arteries located at their edges. The direction of the sector beam is tilted upwards from the root of the nose to the frontal prominence to enable the visualisation of the typical colour Doppler Y-shaped image of the V4 segments at their confluence in the basilar artery [Figure 21].

Figure 21 Typical power Doppler imaging Y-shaped appearance of the distal segments of the vertebral arteries (V4) where they join to form the basilar artery. The depth of insonation of the vertebrobasilar junction usually ranges between 70 and 95 mm.

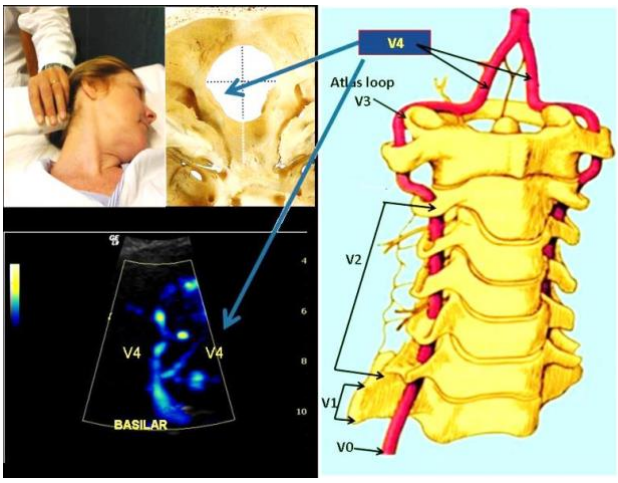

In healthy subjects all segments demonstrate flow away from the transducer. The origin of the basilar artery can be visually identified at a 65 to 70 mm depth; the depth of its superior intracranial end ranges from 95 to 125 mm. Very rarely, the vertebral artery may end in the posterior inferior cerebellar artery (PICA) rather than joining the contralateral VA.

Normal findings

The VA waveform shows a typical low-resistance, continuous and monophasic pattern [Figure 19]. The peak systolic velocity in the vertebral artery can be very variable; it should exhibit a similar shape but a lower velocity than the internal carotid artery. VA PSV ranges from 20 to 60 cm/s, while end-diastolic velocity values range between 5 to 30 cm/s. The resistive index varies from 0.62 to 0.75 [(52)]. The normal diameter of the vertebral artery is

3 to 5 mm. In the presence of hypoplasia, the contralateral artery may exhibit a compensatory hyperplasia and a greater than 2 mm difference between the diameters of the two sides is not uncommon. Almost 50% of patients have a dominant vertebral artery with higher flows than the smaller one; the smaller size non-dominant artery often shows a flow pattern of increased vascular resistance and a decrease in both peak and diastolic velocity [(48)].

The occurrence of a stenotic lesion of the V2 segment is rare and when present the same criteria as the V0 segment are applied. Most turbulence in V2 is due to a vascular tortuosity. Rarely, high-velocity turbulent flow patterns may be detected in the mid segment of a vertebral artery because of extrinsic compression from the vertebrae (often associated with changes in head or neck position). Nonetheless, the examination of the velocity profile of the V2 segment is very important since the finding of a 'tardus parvus' waveform suggests a haemodynamic stenosis within the more proximal segments (V0 or V1).

Common distribution of the obstructive lesions of the vertebral arteries

Stenoses and occlusions of the vertebral arteries are mostly found at the origin (V0) or the intracranial segment (V4) [(51, 53)]. Dissections occur with declining frequency in V3, V2 and V1 [(45)].

V4 vertebral artery stenosis

The threshold value for a >50% stenosis of the intracranial VA is 120 cm/s with reported 100% sensitivity, specificity and positive and negative predictive values [(51)]. The colour Doppler flow appearance of a focal stenosis can be readily visualised by colour flow imaging and confirmed by pulsed wave Doppler [Figure 22].

Figure 22 A high PSV (>2.0 m/s) was detected by spectral doppler interrogation of the left vertebral-basilar junction (a,b). The finding explains the high resistance/low velocity spectral Doppler profile of the left distal vertebral artery (c); a low resistance, normal velocity profile is preserved through the right distal vertebral artery (d)

a

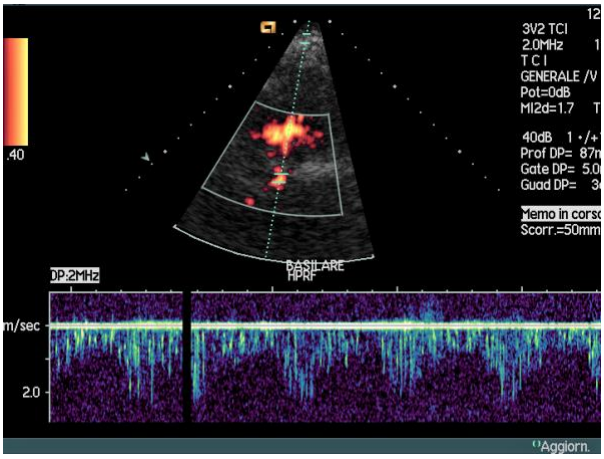

b

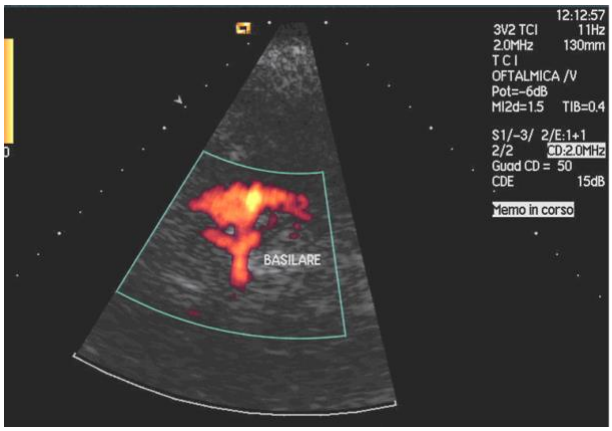

c

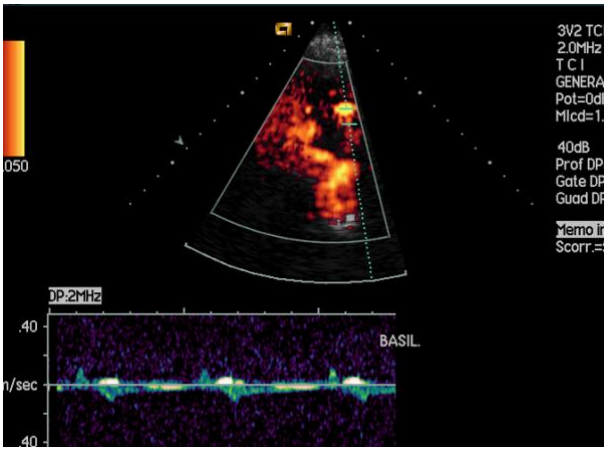

d

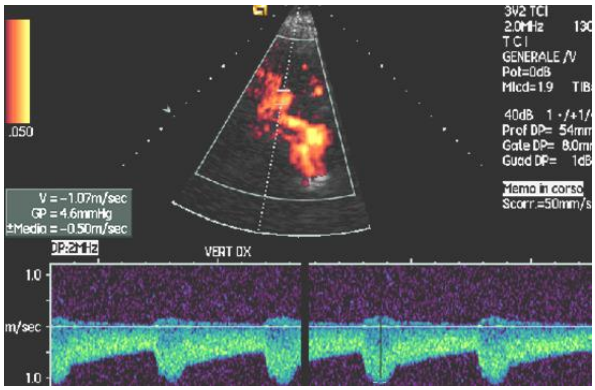

Vertebral occlusion

Transcranial colour coded Doppler (TCCS) accuracy for V4 occlusion is up to 100% [(51)]. The direct evidence of an occlusion of V4 is the lack of colour signal [Figure 23]. The results are very operator dependent and also dependent on the acoustic window. As previously indicated, this finding should not be mistaken with a V4 that continues into the posterior inferior cerebellar artery and this should be excluded. When the occlusion is associated with collateral vessels, the effects on the flow in the downstream waveforms may be extremely variable according to the particular collateral vessels and the location of the obstruction (V0 segment versus V4 segment) [(45)]. Occlusion or a severe stenosis of the V0 segment can create a to and fro or a pulsatile antegrade flow pattern in V4, due to the development of cervical collaterals connecting the vertebral artery with the costocervical and thyrocervical trunks [(45)]. An intracranial V4 occlusion and sometimes a severe stenosis may cause a stump signal or a highly pulsatile flow signal in the upstream V4 portion of the vessel [Figure 22] [(53)].

Figure 23 Power imaging of the vertebrobasilar junction; only the right (RT) V4 segment can be visualised; no flow signal is observed from the left (LT) V4 due to complete occlusion of this segment.

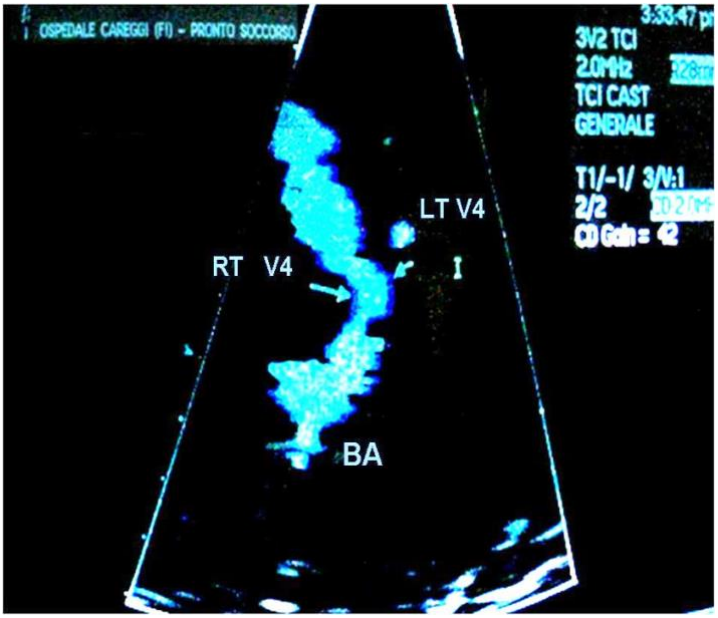

Subclavian steal syndrome

Obstruction of the origin of a subclavian artery is most often the consequence of atherosclerotic disease [(45)]. Complete or incomplete steal may be due to an occlusion or to severe stenosis. Ipsilateral reversal is due to reverse flow from the contralateral vertebral artery since the two vertebral arteries join distally [Figure 24].

Figure 24 Schematic representation of the haemodynamic changes induced by the occlusion of the proximal part of the left subclavian artery; the ipsilateral vertebral artery exhibits an inversion of the flow direction.

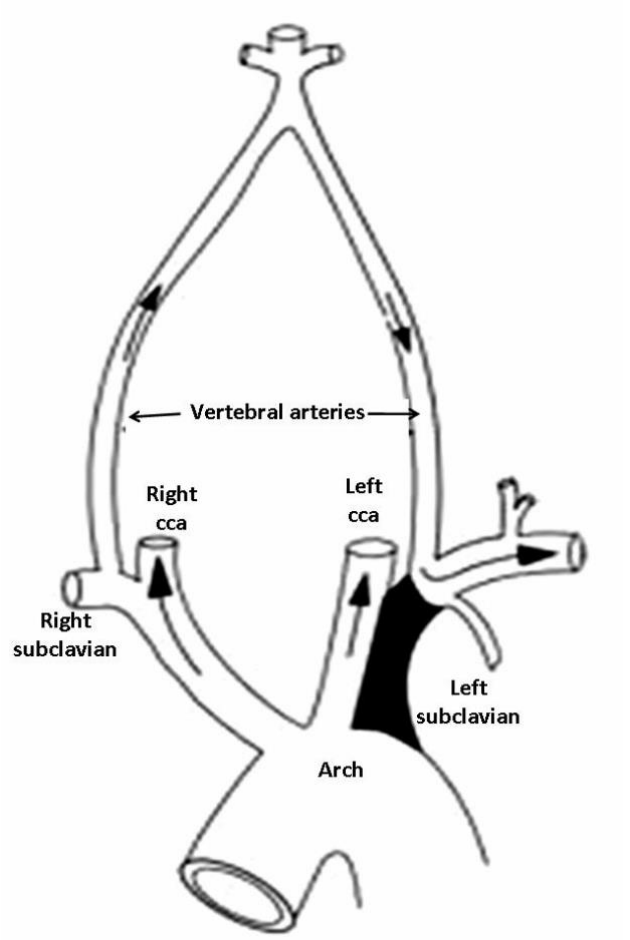

However, other collateral pathways may also be present such as the internal thoracic artery, costocervical trunk or the thyrocervical trunk [Figure 17]. Proximal vertebral disease may also create flow reversal or collateralisation.

The vertebral artery waveform ipsilateral to the steal may be completely reversed or may be incomplete (with a partially reversed component) [Figure 28].

Symptoms are frequently absent [(54)]. Detecting a steal may not have any therapeutic relevance if no neurological symptoms or clinical complaints are present. If present, the clinical signs (dizziness, ataxia and drop attacks) associated with this condition are paradigmatic of vertebrobasilar insufficiency. They typically occur during exertion of the

ipsilateral arm and rarely at rest [(55)]. The progression of a stenosis of the subclavian artery is slow and it is not a common cause of embolic events in the posterior circulation [(49)].

Ultrasound evaluation

The examination of the subclavian artery can be performed by placing a linear transducer on the supraclavicular fossa in a posterior inferior direction. A pulsatile flow away from the transducer and a characteristic velocity reduction during compression of the brachial artery allows prompt vessel identification. The velocity profile has a characteristic muscular high resistance pattern. Right sided stenoses are more readily visible due to the more superficial location of the subclavian arteries. However, most stenoses (85%) occur on the left side [(56)]. When the lumen is visibly narrowed on the B-mode image and aliasing is detected using colour Doppler flow the pulsed wave Doppler waveform can demonstrate high systolic velocity values at the site of the stenosis [Figure 25].

The diagnosis of a subclavian steal is frequently uncovered after detecting an abnormal vertebral waveform and extending the examination to the subclavian arteries [Figure 28].

Figure 25 Narrowing and aliasing is detected by colour-flow examination of the proximal subclavian artery (b) at the site of lumen reduction (a). The spectral Doppler sampling (d) shows an increase in peak systolic velocity. The angiography confirmed the ultrasound finding (c).

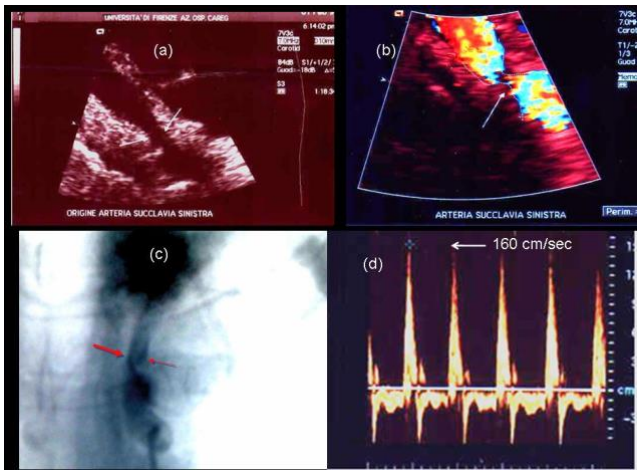

An alternative acoustic window can sometimes be obtained using a phased array at the supra jugular level. The transducer must be first rotated clockwise, toward the left shoulder and tilted slightly downwards; this makes it possible to obtain the aortic arch and the origin of the brachiocephalic trunk, the left common carotid artery and the subclavian arteries in a single view [Figure 26].

Figure 26 2D representation of the thoracic aortic arch (AOB) by the transjugular approach. Ascending aorta (AA); left common carotid (ACC) and left subclavian arteries (AS); descending aorta (AD); main bronchus shadowing (HB); anonymous vein (VA); pulmonary trunk (TP).

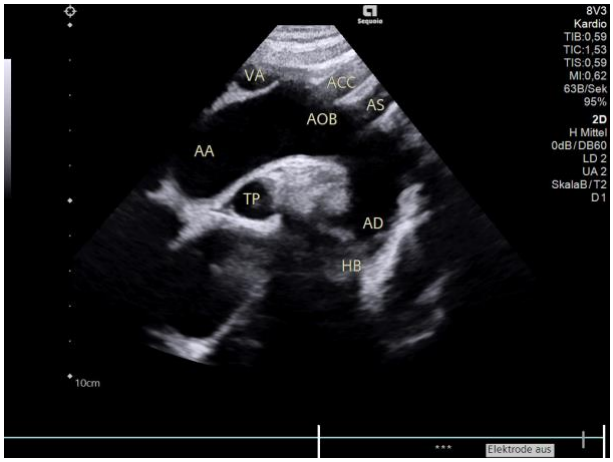

Although the transjugular acoustic window is unsatisfactory in many patients, when obstructive lesions can be visualised this adds useful information [Figure 25-27].

Figure 27 **Colour flow representation of the origin of the left common carotid and left subclavian artery from the aortic arch (transjugular approach). The subclavian artery shows an extensive diameter reduction and extensive intraluminal aliasing due to stenosis.**

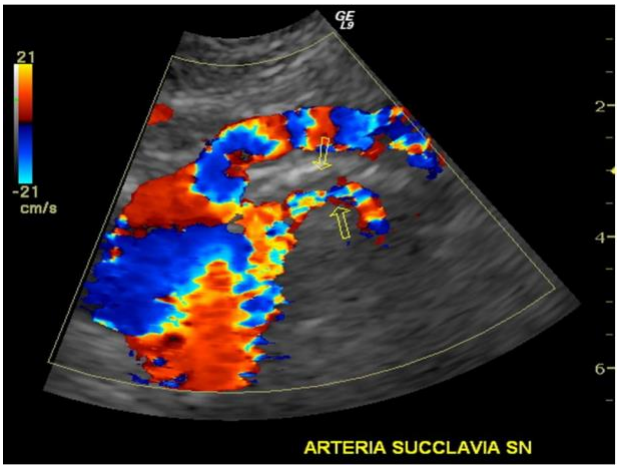

Figure 28 **Incomplete subclavian steal. Transcranial transforaminal view of subclavian steal: the distal segment of the right vertebral artery (V4) coloured in red (a) was consistent with an inversion of arterial flow. The finding was confirmed by the partial flow reversal in the V2 segment (spectral Doppler) (b,d) and was associated with a focal acceleration of blood flow of the proximal subclavian artery due to stenosis (c).**

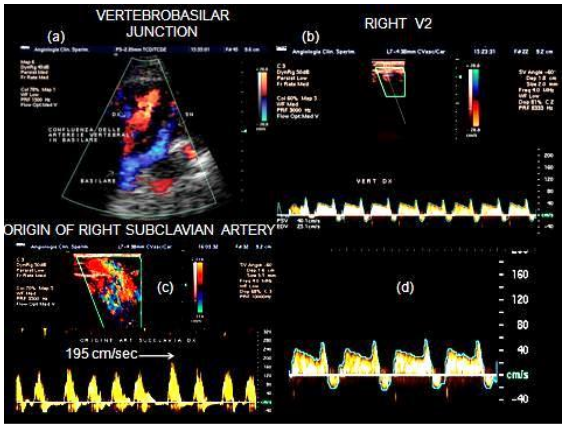

Depending on disease severity, the reversed component can vary; it may vary from an accentuated notch (‘early systolic hesitation’), to a to- and fro flow (with retrograde systolic flow and antegrade diastolic flow), to complete retrograde flow [Figure 29].

Figure 29 The spectral profile of the vertebral artery with early systolic reverse. Progressive increase in duration of systolic flow inversion from (a) to (e) is usually associated with different degrees of collateralisation provided by the contralateral vertebral artery or to different degrees of subclavian stenosis.

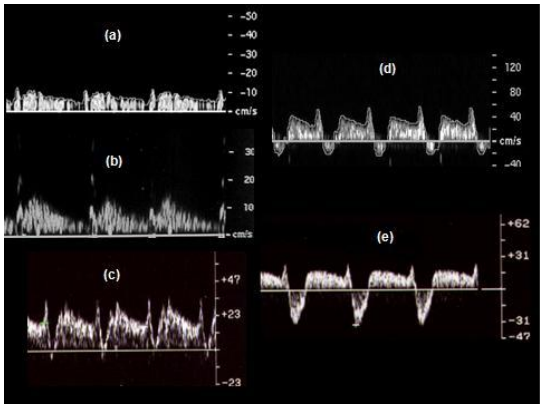

An increase in steal may be deliberately provoked during the hyperaemic reaction following a short period of ischaemia of the arm. The post ischaemic provocative test is performed by inflating an arm cuff (>200 mmHg) for 3 minutes, followed by rapid cuff-release [Figure 30]. When at baseline, the vertebral velocity profile shows an only partial systolic reverse, the demonstration of more pronounced changes in the duration of the retrograde flow in the post-ischaemic phase confirms the diagnosis of subclavian steal syndrome

Figure 30 Post-ischaemic provocative test. The velocity profile of the vertebral artery becomes negative (b) after the release of the arm-cuff and confirms a steal phenomenon caused by a significant obstruction of the subclavian artery.

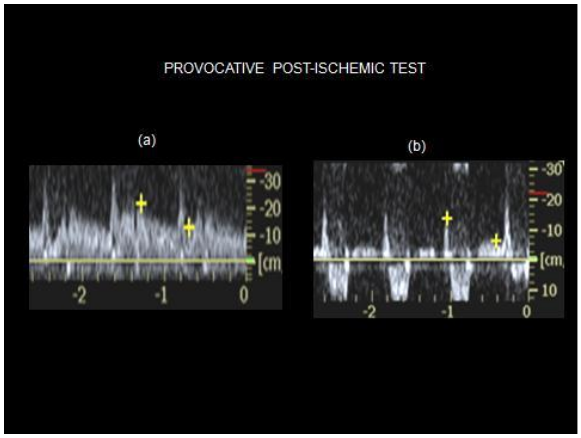

Conclusion

Ultrasound remains a first line diagnostic tool for the evaluation of atherosclerotic disease of the carotid and vertebral arteries. In experienced hands it can provide valuable information for the diagnosis and surveillance of vascular pathologies. The accuracy, reproducibility and reliability of the examination require an appropriate learning curve and knowledge of the anatomy of the intra and extracranial circulation. The best results may be obtained when the operator is fully aware of the strengths of the test but also of its pitfalls and limitations.

References

1. Risk of stroke in the distribution of an asymptomatic carotid artery. The European Carotid Surgery Trialists Collaborative Group. Lancet 1995;345:209-212.

2. North American Symptomatic Carotid Endarterectomy Trial C, Barnett HJM, Taylor DW, Haynes RB, Sackett DL, Peerless SJ, Ferguson GG, et al. Beneficial effect of carotid endarterectomy in symptomatic patients with high-grade carotid stenosis. N Engl J Med 1991;325:445-453.

3. Naylor AR. The importance of initiating "best medical therapy" and intervening as soon as possible in patients with symptomatic carotid artery disease: time for a radical rethink of practice. J Cardiovasc Surg (Torino) 2009;50:773-782.

4. Naylor AR. Time is brain! Surgeon 2007;5:23-30.

5. Naylor AR, Rothwell PM, Bell PR. Overview of the principal results and secondary analyses from the European and North American randomised trials of endarterectomy for symptomatic carotid stenosis. Eur J Vasc Endovasc Surg 2003;26:115-129.

6. Rothwell PM, Gutnikov SA, Warlow CP, European Carotid Surgery Trialist's C. Reanalysis of the final results of the European Carotid Surgery Trial. Stroke 2003;34:514-523.

7. Nicolaides AN, Shifrin EG, Bradbury A, Dhanjil S, Griffin M, Belcaro G, Williams M. Angiographic and duplex grading of internal carotid stenosis: can we overcome the confusion? J Endovasc Surg 1996;3:158-165.

8. Oates CP, Naylor AR, Hartshorne T, Charles SM, Fail T, Humphries K, Aslam M, et al. Joint recommendations for reporting carotid ultrasound investigations in the United Kingdom. Eur J Vasc Endovasc Surg 2009;37:251-261.

9. Jahromi AS, Cina CS, Liu Y, Clase CM. Sensitivity and specificity of color duplex ultrasound measurement in the estimation of internal carotid artery stenosis: a systematic review and meta-analysis. J Vasc Surg 2005;41:962-972.

10. von Reutern GM, Goertler MW, Bornstein NM, Del Sette M, Evans DH, Hetzel A, Kaps M, et al. Grading carotid stenosis using ultrasonic methods. Stroke 2012;43:916-921.

11. Eliasziw M, Rankin RN, Fox AJ, Haynes RB, Barnett HJ. Accuracy and prognostic consequences of ultrasonography in identifying severe carotid artery stenosis. North American Symptomatic Carotid Endarterectomy Trial (NASCET) Group. Stroke 1995;26:1747-1752.

12. Grant EG, Benson CB, Moneta GL, Alexandrov AV, Baker JD, Bluth EI, Carroll BA, et al. Carotid artery stenosis: gray-scale and Doppler US diagnosis--Society of Radiologists in Ultrasound Consensus Conference. Radiology 2003;229:340-346.

13. Qureshi AI, Alexandrov AV, Tegeler CH, Hobson RW, 2nd, Dennis Baker J, Hopkins LN, American Society of N, et al. Guidelines for screening of extracranial carotid artery disease: a statement for healthcare professionals from the multidisciplinary practice guidelines committee of the American Society of Neuroimaging; cosponsored by the Society of Vascular and Interventional Neurology. J Neuroimaging 2007;17:19-47.

14. Nguyen BM, Lin KW, Mishori R. Public health implications of overscreening for carotid artery stenosis, prediabetes, and thyroid cancer. Public Health Rev 2018;39:18.

15. Naidich JB, Weiss A, Grimaldi GM, Kohn N, Naidich JJ, Pellerito JS. Carotid Ultrasound Examinations: Indications Correlated With Abnormal Findings. Ultrasound Q 2018;34:183-189.

16. AIUM Practice Parameter for the Performance of an Ultrasound Examination of the Extracranial Cerebrovascular System 2016.

17. O'Leary DH, Polak JF, Kronmal RA, Manolio TA, Burke GL, Wolfson SK, Jr. Carotid-artery intima and media thickness as a risk factor for myocardial infarction and stroke in older adults. Cardiovascular Health Study Collaborative Research Group. N Engl J Med 1999;340:14-22.

18. Prati P, Tosetto A, Vanuzzo D, Bader G, Casaroli M, Canciani L, Castellani S, et al. Carotid intima media thickness and plaques can predict the occurrence of ischemic cerebrovascular events. Stroke 2008;39:2470-2476.

19. Touboul PJ, Hennerici MG, Meairs S, Adams H, Amarenco P, Desvarieux M, Ebrahim S, et al. Mannheim intima-media thickness consensus. Cerebrovasc Dis 2004;18:346-349.

20. Naqvi TZ, Lee M. Carotid Intima-Media Thickness and Plaque in Cardiovascular Risk Assessment Cardiovascular Imaging 2014;7.

21. Howard G, Sharrett AR, Heiss G, Evans GW, Chambless LE, Riley WA, Burke GL. Carotid artery intimal-medial thickness distribution in general populations as evaluated by B-mode ultrasound. ARIC Investigators. Stroke 1993;24:1297-1304.

22. Ratliff DA, Gallagher PJ, Hames TK, Humphries KN, Webster JH, Chant AD. Characterisation of carotid artery disease: comparison of duplex scanning with histology. Ultrasound Med Biol 1985;11:835-840.

23. Hatsukami TS, Ferguson MS, Beach KW, Gordon D, Detmer P, Burns D, Alpers C, et al. Carotid plaque morphology and clinical events. Stroke 1997;28:95-100.

24. Wolverson MK, Bashiti HM, Peterson GJ. Ultrasonic tissue characterization of atheromatous plaques using a high resolution real time scanner. Ultrasound Med Biol 1983;9:599-609.

25. Zwiebel WJ: Ultrasound Assessment of carotid plaque In: Zwiebel WJ, Pellerito JS, eds. Introduction to Vascular Ultrasonography, Fifth Edition. China: Elsevier Saunders, 2005; 155-159.

26. Mayor I, Momjian S, Lalive P, Sztajzel R. Carotid plaque: comparison between visual and grey-scale median analysis. Ultrasound Med Biol 2003;29:961-966.

27. DeBray JM, Baud JM, Dauzat M. On behalf of the Consensus Conference Consensus concerning the morphology and the risk of carotid plaques. Cerebrovasc Dis 1997;7:289-296.

28. Gray-Weale AC, Graham JC, Burnett JR, Byrne K, Lusby RJ. Carotid artery atheroma: comparison of preoperative B-mode ultrasound appearance with carotid endarterectomy specimen pathology. J Cardiovasc Surg (Torino) 1988;29:676-681.

29. Geroulakos G, Ramaswami G, Nicolaides A, James K, Labropoulos N, Belcaro G, Holloway M. Characterization of symptomatic and asymptomatic carotid plaques using high-resolution real-time ultrasonography. Br J Surg 1993;80:1274-1277.

30. Biasi GM, Froio A, Diethrich EB, Deleo G, Galimberti S, Mingazzini P, Nicolaides AN, et al. Carotid plaque echolucency increases the risk of stroke in carotid stenting: the Imaging in Carotid Angioplasty and Risk of Stroke (ICAROS) study. Circulation 2004;110:756-762.

31. Kakkos SK, Stevens JM, Nicolaides AN, Kyriacou E, Pattichis CS, Geroulakos G, Thomas D. Texture analysis of ultrasonic images of symptomatic carotid plaques can identify those plaques associated with ipsilateral embolic brain infarction. Eur J Vasc Endovasc Surg 2007;33:422-429.

32. Castellani S, Gori F, Battaglia F, Barbanti E, Gensini GF, Pratesi C. Echographic evidence of atheromatous neovascularization is consistent with histological findings and is associated with intraplaque inflammatory cells. Cerebrovasc Dis 2001;11:50.

33. Castellani S, Corsoni V, Zeloni C, Pratesi C, Gensini GF. Echografic evidence of carotid atherosclerotic plaque’s neovascularization. Echographic evidence of carotid atherosclerotic plaque's neovascularization Cerebrovasc. Dis. 1999;9.

34. Staub D, Patel MB, Tibrewala A, Ludden D, Johnson M, Espinosa P, Coll B, et al. Vasa vasorum and plaque neovascularization on contrast-enhanced carotid ultrasound imaging correlates with cardiovascular disease and past cardiovascular events. Stroke 2010;41:41-47.

35. Spencer MP. Full capability Doppler diagnosis. In: Spencer MP, Reed JM, editors. Cerebrovascular Evaluation with Doppler Ultrasound. Netherlands: Martinus Nijhoff 1981.

36. Wardlaw JM, Chappell FM, Best JJ, Wartolowska K, Berry E, Research NHS, Development Health Technology Assessment Carotid Stenosis Imaging G. Non-invasive imaging compared with intra-arterial angiography in the diagnosis of symptomatic carotid stenosis: a meta-analysis. Lancet 2006;367:1503-1512.

37. Faught WE, Mattos MA, van Bemmelen PS, Hodgson KJ, Barkmeier LD, Ramsey DE, Sumner DS. Color-flow duplex scanning of carotid arteries: new velocity criteria based on receiver operator characteristic analysis for threshold stenoses used in the symptomatic and asymptomatic carotid trials. J Vasc Surg 1994;19:818-827; discussion 827-818.

38. Grant EG, Duerinckx AJ, El Saden SM, Melany ML, Hathout GM, Zimmerman PT, Marumoto AK, et al. Ability to use duplex US to quantify internal carotid arterial stenoses: fact or fiction? Radiology 2000;214:247-252.

39. Neale ML, Chambers JL, Kelly AT, Connard S, Lawton MA, Roche J, Appleberg M. Reappraisal of duplex criteria to assess significant carotid stenosis with special reference to reports from the North American Symptomatic Carotid Endarterectomy Trial and the European Carotid Surgery Trial. J Vasc Surg 1994;20:642-649.

40. Polak JF, Bajakian RL, O'Leary DH, Anderson MR, Donaldson MC, Jolesz FA. Detection of internal carotid artery stenosis: comparison of MR angiography, color Doppler sonography, and arteriography. Radiology 1992;182:35-40.

41. Sidhu PS, Allan PL. Ultrasound assessment of internal carotid artery stenosis. Clin Radiol 1997;52:654-658.

42. Riles TS, Lee V, Cheever D, Stableford J, Rockman CB. Clinical course of asymptomatic patients with carotid duplex scan end diastolic velocities of 100 to 124 centimeters per second. J Vasc Surg 2010;52:914-919, 919 e911.

43. Barlinn K, Floegel T, Kitzler HH, Kepplinger J, Siepmann T, Pallesen LP, Bodechtel U, et al. Multi-parametric ultrasound criteria for internal carotid artery disease-comparison with CT angiography. Neuroradiology 2016;58:845-851.

44. Moneta GL, Edwards JM, Chitwood RW, Taylor LM, Jr., Lee RW, Cummings CA, Porter JM. Correlation of North American Symptomatic Carotid Endarterectomy Trial (NASCET) angiographic definition of 70% to 99% internal carotid artery stenosis with duplex scanning. J Vasc Surg 1993;17:152-157; discussion 157-159.

45. von Budingen HC, Staudacher T, von Budingen HJ. Ultrasound diagnostics of the vertebrobasilar system. Front Neurol Neurosci 2006;21:57-69.

46. Grad A, Baloh RW. Vertigo of vascular origin. Clinical and electronystagmographic features in 84 cases. Arch Neurol 1989;46:281-284.

47. Moubayed SP, Saliba I. Vertebrobasilar insufficiency presenting as isolated positional vertigo or dizziness: a double-blind retrospective cohort study. Laryngoscope 2009;119:2071-2076.

48. Dietrich EB. Normal cerebrovascular anatomy and collateral pathways. In: Zweibel WJ, Pellerito JS, editors. Introduction to vascular ultrasonography. Philadelphia: ELSEVIER SAUNDERS; 2005. p. 133-154.

49. Caplan LR, Wityk RJ, Glass TA, Tapia J, Pazdera L, Chang HM, Teal P, et al. New England Medical Center Posterior Circulation registry. Ann Neurol 2004;56:389-398.

50. Bendick PJ, Jackson VP. Evaluation of the vertebral arteries with duplex sonography. J Vasc Surg 1986;3:523-530.

51. Baumgartner RW, Mattle HP, Schroth G. Assessment of >/=50% and <50% intracranial stenoses by transcranial color-coded duplex sonography. Stroke 1999;30:87-92.

52. Trattnig S, Hubsch P, Schuster H, Polzleitner D. Color-coded Doppler imaging of normal vertebral arteries. Stroke 1990;21:1222-1225.

53. Schaeberle W. Extracranial arteries supplying the brain In Ultrasonography in vascular diagnosis. Berlin, Heidelberg: Springer-Verlag, 2005: 207-251.

54. Ackermann H, Diener HC, Dichgans J. Stenosis and occlusion of the subclavian artery: ultrasonographic and clinical findings. J Neurol 1987;234:396-400.

55. Fields WS, Lemak NA. Joint Study of extracranial arterial occlusion. VII. Subclavian steal--a review of 168 cases. JAMA 1972;222:1139-1143.

56. Talbot SR, Zweibel WJ: Assessment of upper extremity arterial occlusive disease. In: Zweibel WJ, Pellerito J, eds. Introduction to vascular ultrasonography. Philadelphia: ELSEVIER SAUNDERS, 2005; 297-323.